THE HIP-SPINE EFFECT: HOW PATHOLOGICAL FEMORO-PELVIC INTERACTIONS CONTRIBUTE TO ABNORMAL LUMBAR SPINE LOADING

By

ANTHONY NICHOLAS KHOURY, M.S

Presented to the Faculty of the Graduate School of

The University of Texas at Arlington in Partial Fulfillment

of the Requirements

for the Degree of

DOCTOR OF PHILOSOPHY

THE UNIVERSITY OF TEXAS AT ARLINGTON

May 2019

Supervising Committee:

Hal David Martin, D.O: Supervising Professor

Cheng-Jen Chuong, Ph.D: Co-Supervising Professor

Jun Liao, Ph.D.

Kent Lawrence, Ph.D.

ACKNOWLEDGEMENTS

I would first like to express my deepest appreciation to my supervising professor Dr. Hal David Martin. I am grateful for the opportunity you provided me and for all the guidance, support, and lessons you have instilled over the years. Thank you for helping me to become a better investigator and fortifying my passion for research and helping others. A sincere thank you to Dr. Cheng-Jen Chuong for guiding me through the PhD process and providing the resources to accomplish the research goals with the Hip Preservation Center. I would also like to thank my committee members including Dr. Kent Lawrence and Dr. Jun Liao for their instruction and supervision throughout the finite element analysis objectives.

This work would not have been completed without Dr. Juan Gomez-Hoyos and Ricardo Schroder. I am extremely grateful for their friendship and mentorship throughout this graduate experience. Their passion for research and advancing science has inspired me throughout the years and they have taught me everything I know about the hip and conducting good research. I am especially thankful to Tejas Mhetre for his assistance with developing the finite element models.

Finally, I would like to thank the Baylor Research Institute for their research support. Additionally, I am thankful for UT Southwestern Willed Body Program and United Tissue Network for supplying the specimens necessary to complete the cadaveric experiments in addition to those who have donated themselves to science. This selfless act and subsequent research findings have enriched the lives of countless people today and will continue to do so in the future.

May 2, 2019

DEDICATION

I dedicate this dissertation to my loving wife and family. Thank you for your boundless patience, understanding and love during this process. Megan, you have stood by my side throughout this journey and you continue to inspire me every day. I am especially thankful for my family, Mary Ann, Anton, and Kristen. Your endless guidance and support have propelled me to where I am today.

ABSTRACT

THE HIP-SPINE EFFECT: HOW PATHOLOGICAL FEMORO-PELVIC INTERACTIONS CONTRIBUTE TO ABNORMAL LUMBAR SPINE LOADING

Anthony Nicholas Khoury, Ph.D.

The University of Texas at Arlington, 2019

Supervising Professor: Hal David Martin

Cheng-Jen Chuong

Lumbar pathology has been shown to explain hip pain, as hip pathology is involved in the development of lumbar pain by the disruption of normal lumbopelvic kinematics. Hip pathologies that contribute to lumbar pain include flexion deformities, osteoarthritis, congenital hip dislocation, and limited hip range of motion. To date there is a paucity of research that actively looks to investigate the symbiotic relationship between the hip and the spine. Specific pathologies and treatment methods have largely focused on the individual components without considering the global effects of the structures involved. The biomechanics of hip pathology must be studied in depth in order to provide a discreet knowledge of diseases.

Ischiofemoral impingement, femoroacetabular impingement, and femoral version are commonly diagnosed and treated hip pathologies, however altered biomechanics are poorly understood. The hypothesis states lumbar pain can be generated by increased force transmission through the spine as a result of abnormal hip anatomy during normal gait movement of hip flexion and extension. Ischiofemoral impingement, femoroacetabular impingement, and femoral

version will have a positive impact on force generation to the lumbar spine region, ultimately resulting in primary pain complaints. The biomechanical effects of these specified abnormal hip pathologies on the lumbar spine will be investigated with the development of novel cadaveric pathology simulations. The lumbar spine loading will be further studied using a developed Finite Element Analysis model to further quantify the underlying biomechanics.

Three analytical techniques were utilized to quantify the relationship between the hip pathologies and lumbar pain. 1) The hip pathologies investigated were reproduced in a cadaveric model and tested in various phases of hip extension and flexion and compared to native hip anatomy. The cadaveric model provides a reasonable medium for testing due to real-life conditions and variability within samples that reflect a more normal population. 2) Gait analysis techniques were utilized to study specific lumbopelvic motion in decreased femoral version cases. 3) Finite Element Analysis models were then created to simulate normal and pathological hip conditions and tested in the corresponding hip flexion and extension movements. Regional deformation and load change in the lumbar region as a consequence of abnormal hip anatomy will provide valuable information on how the hip affects the spine.

Cadaveric experiments to simulate the related hip pathologies proved successful in establishing a direct kinematic chain link between abnormal hip pathology and the lumbar spine. Simulated ischiofemoral impingement increased L3-4, L4-5, and L5-S1 facet joint loading during 10° and 20° hip extension, when compared to native hip specimens. Simulated cam-type femoroacetabular impingement displayed similar results. An increase in L3, L4, and L5 intervertebral disk loading was observed in the presence of anterior hip impingement, when compared to normal hips. Abnormal femoral version experiments produced interesting data during which decreased femoral version (-10°) reduced lumbar facet joint loading when

compared to native hip specimens. Conversely, increased femoral version (+30°) elevated lumbar facet joint loading when compared to native hips. A gait study investigating patients with imaging-based confirmed decreased femoral version resulted in significant differences in lumbopelvic movement and ground reaction force when compared to healthy individuals. The finite element analysis models developed accurately reflected similar trends in lumbar loading increase or decrease during hip flexion and extension.

The resultant data obtained from cadaveric benchtop experiments, gait/motion analysis, retrospective clinical studies, and finite element analysis confirms the deleterious impact abnormal hip pathology has on the lumbar spine. The excessive loading experienced within the lumbar spine, due to abnormal hip pathology, generates primary low back pain complaints. Examination of the hip joint anatomy is imperative during low back physical examination to investigate any deviations within the kinematic chain. The advanced understanding of these hip pathologies allows for more comprehensive surgical and conservative treatment planning.

TABLE OF CONTENTS

LIST OF FIGURES

LIST OF TABLES

Chapter 1

Introduction

1.1 The hip and lumbar spine

Lumbar spine pain is an epidemic with an estimated 80% of the population complaining of symptoms.[1] The complex nature of the pathology and confounding variables that attribute to the pain are poorly understood. In the United States, more than 1.5 million lumbar magnetic resonance imaging studies are performed every year, with 300,000 reporting nerve root compression and only 200,000 patients obtaining relief from discectomies and other surgeries directed at relieving pressure on the spinal roots[2]. Physicians who treat patients spinal-related complaints should recognize that other Orthopaedic diagnoses involving the hip or lower limb are present in approximately 86% of the cases.[2]

The high prevalence of low back pain in the population results in a high level of cost for treatment. Currently the symptoms are the most frequent motive for consultation, generally treated by both Orthopaedic Surgeons and Neurosurgeons. Low back pain treatment varies depending on the surgical discipline consulted; however, the majority of patients displays no abnormalities on MRI and do not achieve pain relief from procedures directed at alleviating pressure on the spinal roots.[2]

1.1.1 Hip-Spine Syndrome

The first description of a coexistence between lumbar pain and hip abnormalities was produced by Offierski in 1983.[3] Lumbar pathology has been shown to explain hip pain, as hip pathology has been involved in the development of lumbar pain by the disruption of normal lumbopelvic

kinematics. Hip pathologies that contribute to lumbar pain include flexion deformities[3], osteoarthritis[4,5], congenital hip dislocation[6], and limited hip range of motion.[7,8] To date no proper studies have been developed to investigate the biomechanical relationship between abnormal hip disorders and lumbar spine kinematics.

1.1.2 Five level approach to understanding hip and lumbar spine pain

Accurate assessment of the hip joint requires a multi-level approach that takes into consideration the numerous structures surrounding the hip. These levels include the: 1) osseous 2) capsulolabral 3) musculotendinous 4) neurovascular 5) kinematic chain. The kinematic chain is the most critical level for advanced understanding of the hip-spine relationship because the hip is the center axis of body movement. Abnormalities in any of the levels of the hip joint affect the overall kinematic chain motion and lead to disruptions in normal movement.

1.1.3 Hip pathology: Osseous impingements

Osseous impingements that restrict normal hip motion include ischiofemoral impingement and Femoroacetabular impingement. Ischiofemoral impingement is characterized as decreased space between the lesser trochanter of the femur and ischium of the pelvis. The smallest distance between these two osseous structures is commonly defined by Magnetic Resonance Imaging. An ischiofemoral space distance less than 17mm is a diagnostic feature for ischiofemoral impingement.[9] Femoroacetabular impingement is an abnormal osseous contact between the proximal femur and acetabular rim that occurs during dynamic hip motion.[10] The pathology exists in two forms: cam impingement and pincer impingement. Cam impingement is characterized by a boney overgrowth along the superior portion of the femoral head, resulting in an increased radius of the femoral neck at the femoral head-neck junction.[11] The cam

impingement produces shear forces which results in an “outside-in” acetabular cartilage damage and labral tears. The cam impingement is more commonly observed in younger, athletic patients. Pincer impingement is a boney overgrowth along the acetabular boarder and is a result of abnormal acetabular development. Similar to the pincer impingement, continued excessive hip movements contributes to labral damage and delamination of cartilage. Pain is associated with these degenerative mechanisms and early onset of osteoarthritis is a significant factor. Cam and pincer impingement can occur independently or as a combination of the two.

1.1.4 Hip pathology: Femoral version

Structural anatomic orientation is a critical factor for proper body function. Similar to the described osseous impingements, any deviations from normal anatomy may have a profound impact on body motion through kinematic chain disturbances. Femoral neck version is the axial orientation of the femoral neck in relation to the horizontal axis of the posterior femoral condyles. For males, normal femoral neck version is anteriorly oriented in 10 degrees; for females 15 degrees. Patients presenting with abnormal femoral neck version have concomitant gait symptoms as a result of rotational misalignment of the lower extremities. Decreased femoral neck version, also referred as femoral retroversion, occurs when the femoral neck version is less than 10 degrees and the femoral head has a posterior projection into the acetabular cup.

1.1.5 The problem

To date there is a paucity of research that actively looks to investigate the symbiotic relationship between the hip and the spine. Specific pathologies and treatment methods have largely focused on the individual components without taking into account the global effects of the structures involved. The biomechanics of hip pathology must be studied in depth in order to provide a

discreet knowledge of diseases. The advanced understanding will allow for more comprehensive surgical and conservative treatment planning, as well as the development of devices that correct the problem at hand effectively and economically.

1.2 Overview of Research Project

Ischiofemoral impingement, femoroacetabular impingement, and femoral version are commonly diagnosed and treated hip pathologies, however altered biomechanics as a result of disease are poorly understood. To fully understand the relationships between these pathologies and lumbar pain cadaveric models have been developed. The cadaveric model provides a reasonable medium for testing due to real-life conditions and variability within samples that reflect a more normal population. Finite element modeling is a useful tool to further validate outcomes of the benchtop cadaveric experimental models. Unfortunately, the intricate musculotendinous and ligamentous anatomy places too much constraint on the general problem at hand. Regional deformation and load change in the lumbar region as a consequence of abnormal hip anatomy will provide valuable information on how the hip affects the spine.

1.2.1 Hypothesis

The hypothesis states that lumbar pain can be generated by increased force transmission through the spine as a result of abnormal hip anatomy during normal gait movement of hip flexion and extension. Ischiofemoral impingement, femoroacetabular impingement, and femoral version will have a positive impact on force generation to the lumbar spine region, ultimately resulting in primary pain complaints.

1.2.2 Specific Research Aims

1. **The effect of ischiofemoral impingement on lumbar facet joint loading**

   Lumbar facet joint loading will be investigated by modeling ischiofemoral impingement in a cadaveric specimen. Loading will be measured during hip extension to 10 and 20 degrees with neutral abduction and compared to the native state.

2. **The effect of cam-type femoroacetabular impingement on intervertebral disk loading**

   Intervertebral disk loading will be measured in the presence of Cam-type anterior femoroacetabular impingement with 90 degrees, 90 + Internal rotation, 120 degrees, 120 + internal rotation, and Impingement test.

3. **The effect of increased and decreased femoral anteversion on the lumbar spine**

3A Increased and decreased femoral version will be simulated in cadaveric specimens and facet joint loading will be measured during hip extension to 10° and 20° with normal abduction

3B Lumbo-pelvic gait changes will be monitored using gait analysis techniques in patients with decreased femoral version compared to normal patients, during a normal gait cycle

4. **Finite element analysis of ischiofemoral impingement, cam-type femoroacetabular impingement, and increased/decreased femoral version**

Chapter 2

Aim 1: The effect of ischiofemoral impingement on lumbar facet joint loading

2.1 Introduction

Since the first description about the clinical importance of lumbar disc herniation in 1934, lower back pain and lower leg symptoms (including posterior hip pain) have been commonly linked to spine problems.[12]

The understanding of hip pain has undergone significant transformation in recent years. The opportunities to improve knowledge at biological, biomechanical, and clinical levels have led to more advance descriptions of intra-articular and extra-articular hip pathologies as a cause of posterior hip pain and sciatica.[13–15]

Lumbar pathology can explain hip pain in a number of cases, and hip pathology has similarly been involved in producing or worsening lower back problems by disturbing the normal lumbopelvic kinematics. A number of hip pathologies such as flexion deformities,[3] osteoarthritis,[4,5] congenital hip dislocation,[6] and limited hip range of motion[7,8] have been linked to lumbar disturbances that produce or worsen lower back pain. This pathologic relation known as "hip-spine syndrome" was first described by Offierski in 1983[3]; however, there have been no biomechanical studies focusing on the influence of hip disorders on lumbar spine kinematics.

Forward pelvic rotation caused by hip pathology produces hyperlordosis of the lumbar spine[3]; this could potentially generate lumbar facet load changes and foramen narrowing. In the presence of limited terminal hip extension during gait produced by an condition, including ischiofemoral impingement (IFI) due to direct contact between the lesser trochanter and the ischium, biomechanical disturbances such as pelvic rotation, pelvic tilt, and axial skeleton

adaptations are created.[16] Secondary pelvic rotation, hyperlordosis, facet joint overload, and foramen narrowing could explain lower back symptoms in patients with IFI or any condition involving limited terminal hip extension.

The purpose of this study was to assess the relation between IFI and lumbar facet joint load during hip extension in cadavers.

The hypothesis states simulated IFI will contribute to increased facet joint loading during hip extension when compared to non-IFI native hips.

2.2 Materials & Methods

2.2.1 Specimens

Sixteen fresh-frozen hip specimens from fresh T1-toe cadavers (no head, no arms) were utilized. The donors included 4 males and 4 females who were 62.4 years of age on average. Specimens were excluded based on visual gross morphologic deformity or pathology (e.g. scoliosis, osteoporotic or metastatic lesions, previous surgeries or trauma, abnormal lumbar lordosis or sacral slope) and computed tomography scan with evidence of any major degenerative disease (osteoporosis, osteoarthritis, etc.). Specimens with soft tissue contracture (positive Thomas test) around the hip were excluded. An Orthopaedic surgeon (JGH) assessed all specimens.

2.2.2 Premeasurement Imaging Evaluation

Axial, coronal, and sagittal computed tomography scan sequences (General Electric Medical Systems, LightSpeed RT16 XTRA, GE Healthcare, Buckinghamshire, United Kingdom) of the spine, pelvis, and lower limbs were performed on all cadavers before biomechanical testing. The

feet were taped in a functional walking position and neutral abduction to simulate real gait conditions and to obtain consistency during imaging assessment. Images were analyzed in GE MediaViewer 5 (GE Healthcare) to calculate the native (original) femoral version and McKibbin's index of the specimens.[17] Hip measures included femoral neck version, acetabular version, lesser trochanteric version, and ischiofemoral space (IFS). (Figure 1)

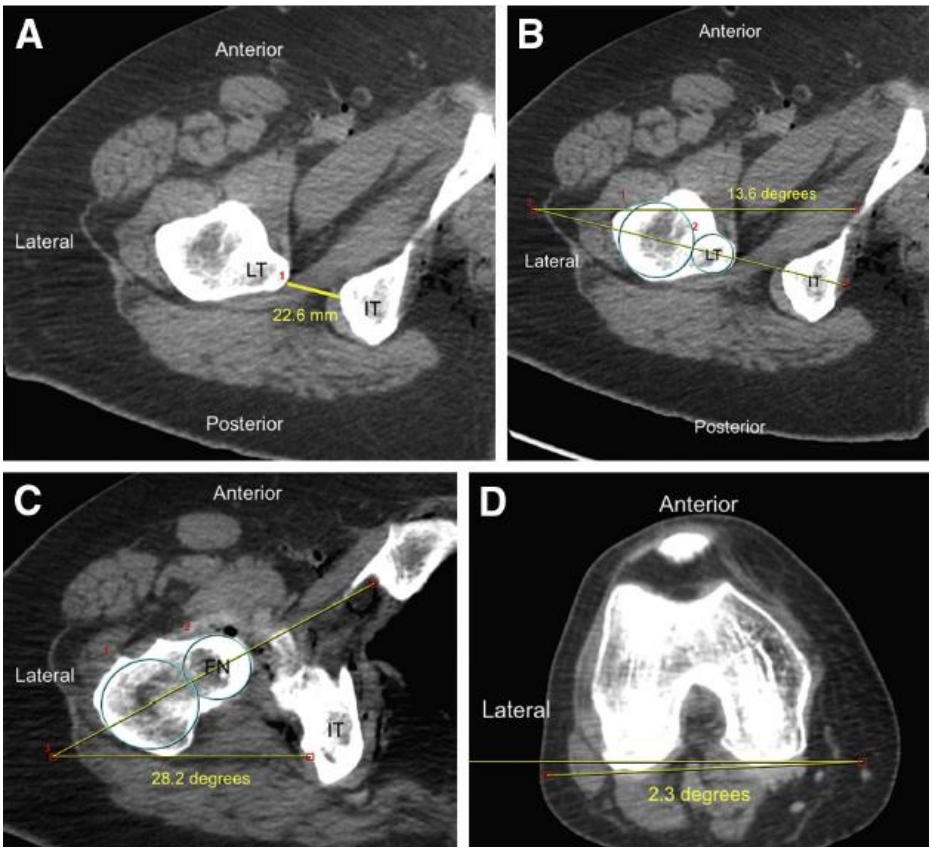

Figure 1 CT Scan Measurements

CT scan measurements. A. Ischiofemoral space was considered as the smallest distance between the lateral cortex of the ischial tuberosity and the medial cortex of the lesser trochanter. B&C For measuring the lesser trochanter version and femoral neck version, two centroids positioned in the body of the lesser trochanter or the femoral neck, one in the midline of the basis and a second one at the border of the tip, as seen in B and C; the angle of the line passing between the middle of both centroids and a horizontal line was called the lesser trochanter axis, or femoral neck axis. D. The angle between the lesser trochanter axis or the femoral neck axis and the posterior condylar axis represented the lesser trochanteric version and femoral neck version, respectively. (FN: femoral neck; IT: ischial tuberosity; LT: lesser trochanter)

Spine measurements were intervertebral L4-L5 angle, sacral slope, and lumbar spine Cobb angles on the frontal and sagittal places.[18] In addition, leg length (from the center of the femoral head to the center of the tibiotalar joint) and knee varus and/or valgus angle were measured.

2.2.3 Specimen Setup

Cadavers were positioned in lateral decubitus on a dissection table. Two fixated boards were positioned anterior to the chest and posterior to the lumbar spine (distal border of the board proximal to L2) to stabilize the upper torso and simulate the normal sagittal balance. The examined leg was placed on the testing frame with the hip joint in a neutral position and the tibiotalar and subtalar joints locked at 90° with a custom-designed foot bracket. The knee was transfixed with two Steinmann pins in 0° extension simulating terminal hip extension during gait. the contralateral leg, locked in the same manner, was placed on the dissection table in 20° of hip flexion and fixated with a Schanz pin (Stryker, Kalamazoo, MI) simulating a normal gait position. (Figure 2)[19]

2.2.4 Surgical Approach and Measurement Methods

A posterior approach to the lumbar spine was performed down the middle of the back through a 20- to 25-cm incision. The fat and lumbodorsal fascia to the spinous process was dissected preserving the interspinous ligament. Paraspinal muscles were detached subperiosteally and dissected down to the spinous process and lamina to the facet joint. The L3-L4 and L4-L5 ipsilateral facet joint capsules were carefully incised approximately 10mm allowing for the placement of an ultrasensitive piezoresistive force sensor (FlexiForce B-201; Tekscan, South Boston, MA). The capsule was not resected to avoid considerable disturbances in facet anatomy or biomechanics. Direct visualization was used as a qualitative indication of sensor placement

and was inspected after each testing condition. (Figure 3) New sensors were used for every specimen and individually calibrated for both the left and right side to convert sensor saturation to Newtons.

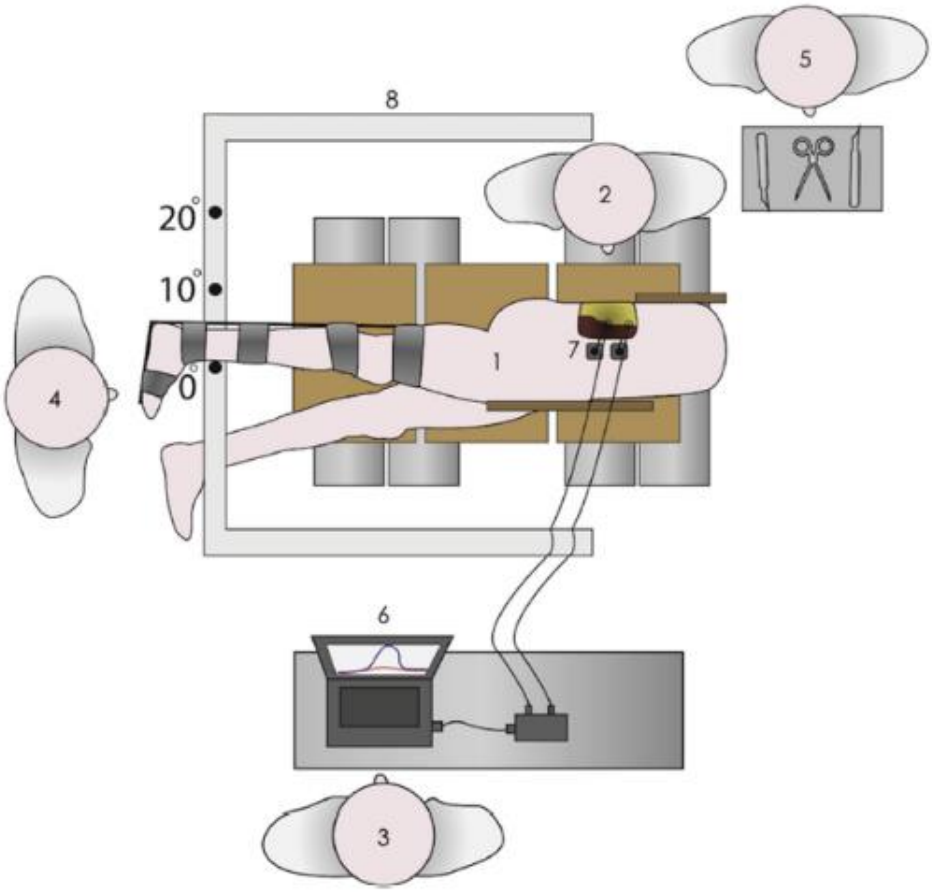

Figure 2 IFI cadaver set up

IFI cadaver set up. Superior view of specimen positioned in lateral decubitus on a dissection table and secured with two fixated boards. The examined leg is placed on the testing frame with the hip joint in a neutral position and the ankle locked at 90°. The knee is fixed with Steinmann pins in neutral extension. The contralateral leg is placed at 20° hip flexion and fixated to the table with Schanz pins. 1, Specimen in lateral position. 2, Orthopaedic surgeon performing a surgical approach and sensor placement. 3, Biomedical engineer operating the force sensor system. 4, Physical therapist performing leg movements for each testing condition. 5, Surgical assistant. 6, Computer registering peak forces in facet joints. 7, Sensors placed into the facet joints. 8, PVC frame

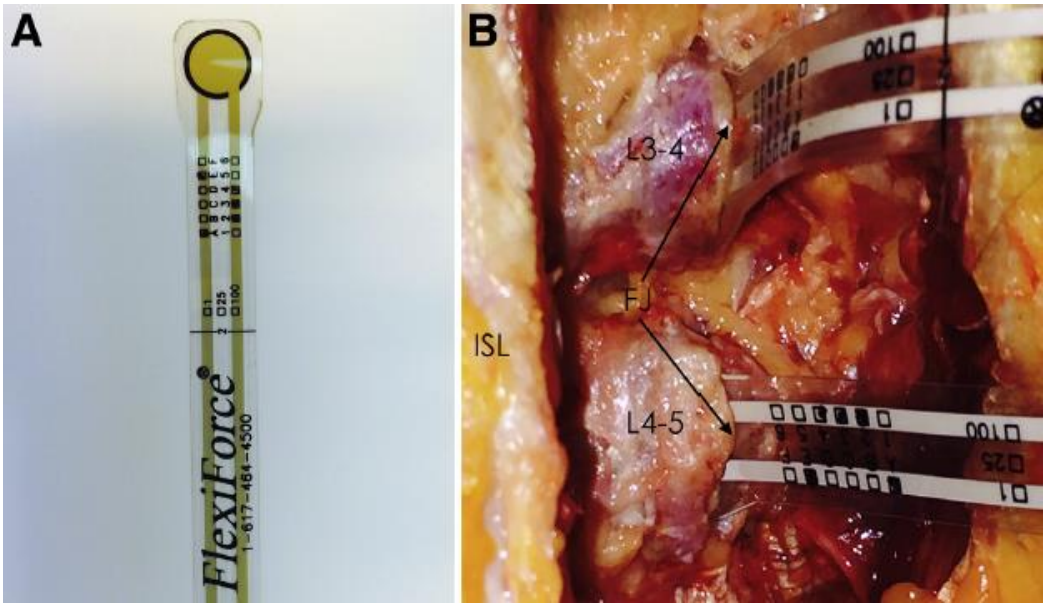

Figure 3 Piezoresistive force sensors

A. Ultrasensitive force sensor FlexiForce B-201 (Tekscan, South Boston, MA). B. Insertion of the sensors into the right L3-L4 and L4-L5 facet joint. (FJ, facet joint. ISL, interspinous ligament)

2.2.5 Ischiofemoral Impingement Model and Testing

A posterolateral approach to the hip was made over the lesser trochanter through a 5- to 7-cm incision. The iliotibial band was identified and incised in line with the skin incision. The gluteus maximus was split and retracted medially and posteriorly to provide access to the IFS.

After dissecting the quadratus femoris muscle, a digital caliper, 0.01mm accuracy (iGaging Inside, San Clemente, CA) was used to measure the native IFS under direct observation in 0° hip extension and 0° hip abduction. Subsequently, an osteotomy at the base of the lesser trochanter was performed and metallic washers (1.6 x 1.5 x 0.1 inches) were inserted into the osteotomy to lengthen the size of the lesser trochanter and get zero IFS to produce impingement. The number of washers was defined according to the native IFS until impingement between the lateral part of the ischium and lesser trochanter. (Figure 4)

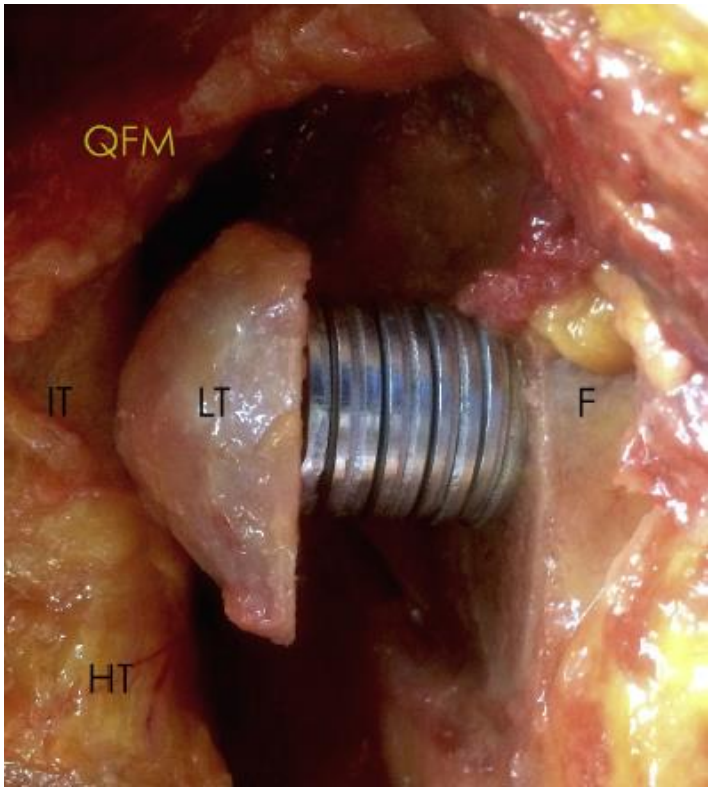

Figure 4 Simulated IFI

Simulated IFI. An osteotomy of the lesser trochanter was performed, and metallic washer were inserted into the osteotomy to increase the lesser trochanter size and reduce the IFS. (F, femur. HT, hamstring tendon origin. IT, ischial tuberosity. LT, lesser trochanter. QFM, quadratus femoris muscle)

The osteotomy and metallic washers were fixed using a cortical 3.5mm screw (Stryker) through the native axis of the lesser trochanter.

2.2.6 Measurements and Hip Positions

A PVC frame was built to provide support to the cadaver leg during the experiment. (Figure 2) The frame was heightened and lowered to provide neutral abduction for each experiment. Neutral abduction was confirmed with a bubble level.

Before all testing condition, 0°, 10°, and 20° hip extension points were marked on the frame based on the center axis of the hip joint. The greater trochanter and lateral condyle of the distal femur were used as landmarks. The angles were measured using a baseline goniometer (White Plains, NY). To permit freedom of motion in the hip joint, no attachments were used during position manipulation.

The leg was preconditioned with 3 cycles from 0° to 20° hip extension. The leg was then moved in testing cycles from 0° to 10° hip extension and from 0° to 20° hip extension. Every cycle was performed in neutral abduction. Abduction was measured with a goniometer by the same examiner for all experiments. The leg was held for 1 second at the starting and final position of each cycle, and the timing was noted for data analysis. Every cycle was repeated 10 times by the same examiner for all experiments, and an average was registered as the final value. All examiner except for the piezoresistive force sensor operator were blinded to the results.

2.2.7 Statistical Analysis

Microsoft Excel (Microsoft, Redmond, VA) was used to compile raw data in addition to calculating the percent change before and after IFI simulation at 10° and 20° hip extension. Statistical analysis was performed using SPSS (V22) (SPSS, Chicago, IL). The Kolmogorov-Smirnov and Shapiro-Wilk tests were used to assess the normal distribution of variables. Z-scores for skewness and kurtosis were calculated and Q-Q plots verified assumption of normality. Mean and standard deviation were used for description of quantitative variables. Four paired t-tests were performed for comparing normal IFS and IFI on the L3-L4 and L4-L5 facet joint loads. Alpha was set at 0.05.

2.3 Results

2.3.1 Cadaver Demographics

Sixteen specimens (8 cadavers) were considered for this study. Two cadavers were excluded (one cadaver used for pilot experimentation and one excluded due to joint contracture). Twelve hips were included were included for final data analysis (6 cadaveric specimens). The donors included 3 males and 3 females 63.8 years of age on average (range, 52-78 years, SD ±8.4) and body mass index was 23.9 on average (range, 19.8-32.8, SD ±5.02).

Femoral neck, acetabular, and lesser trochanteric version were similar between specimens (13.63°, SD ±3.99; 21.22°, SD ±6.34; and -21.30°, SD ±5.43). Native IFS was 17.75 mm (SD ±5.44) on average. Imaging parameters for coronal and sagittal balance of the lumbar spine were consistent. (Table 1)

Table 1 Demographic and imaging characteristics of the specimens used

Parameter	Mean	Minimum	Maximum	Standard Deviation
Age, yr	63.83	52.00	78.00	8.44
Height, inches	66.83	61.00	72.00	4.75
Weight, pounds	155.16	105.00	240.00	49.89
Body mass index	23.96	19.80	32.50	5.02
Leg length, cm	78.95	71.20	88.40	6.80
Femoral neck/shaft angle, °	132.51	128.70	137.00	3.09
Femoral neck version, °	13.63	7.30	20.30	3.99
Acetabular version, °	21.22	12.60	32.00	6.34
McKibbin's index, °	34.85	24.60	47.80	7.74
Lesser trochanteric version, °	−21.30	−28.40	−11.90	5.43
Native ischiofemoral space, mm	17.75	8.40	25.60	5.44
Coronal Cobb angle, °	2.80	0.20	6.20	1.98
Sagittal Cobb angle, °	46.11	23.80	57.20	13.41
Sagittal L4-5 intervertebral angle, °	9.31	8.10	11.70	1.32
Sacral slope, °	41.66	29.00	49.90	7.24
Knee valgus, °	4.50	0.70	6.90	2.12

Native loads for L3-L4 and L4-L5 at 0° hip extension were 25.7 N (SEM ±8.01) and 12.5 (SEM ±3.6), respectively. The average baseline facet joint loads were 41.88 N (SD ±40.83) for L3-L4 at 10° of hip extension and 49.89 N (SD ±48.50) at 20° of hip extension. L4-L5 facet joint loads were 24.03 N (SD ±26.19) for 10° and 34.93 N (SD ±34.11) on average for 20° hip extension. (Figure 5)

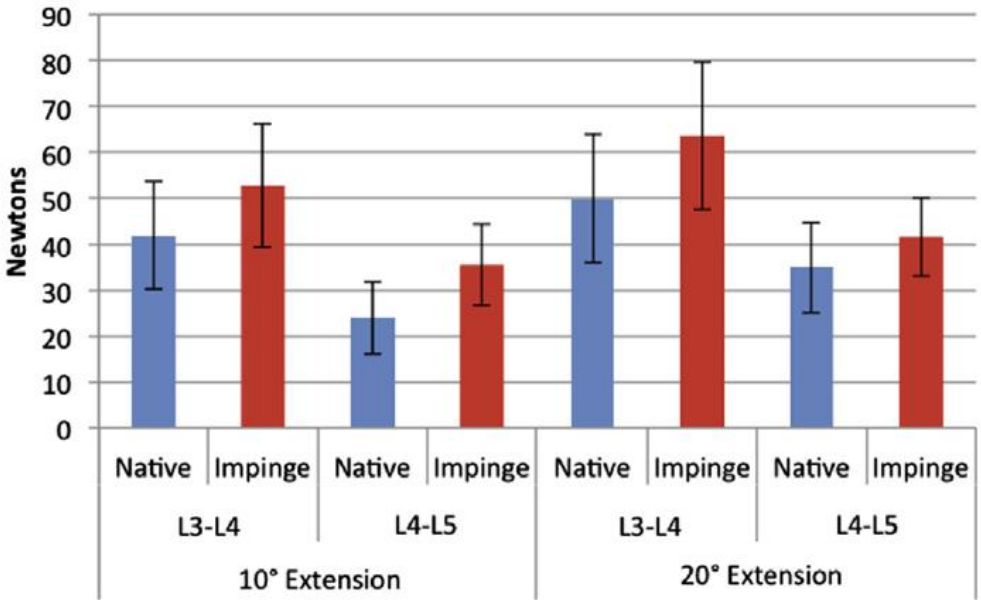

Figure 5 IFI peak facet force

After simulating IFI, mean absolute differences of facet joint load were 10.8 N (SEM ±4.53, $p < 0.036$) for L3-L4 at 10° of hip extension, 13.71 N (SEM ±4.53, $p < 0.012$) for L3-L4 at 20° of hip extension, 11.49 (SEM ±4.33, $p < 0.024$) for L4-L5 at 10° of hip extension, and 6.67 N (SEM ±5.43, $p < 0.245$) for L4-L5 at 20° of hip extension. (Figure 6) Statistical significance ($p < 0.05$) for facet load was found in all parameters except for L4-L5 at 20° of hip extension.

High variability in native facet joint loading was recognized and the average percentage change for L3-L4 and L4-L5 at 10° and 20° of hip extension after simulating IFI was calculated. An average facet joint load of 30.81% (range: 28.16% to 32.07%) was obtained. (Table 2)

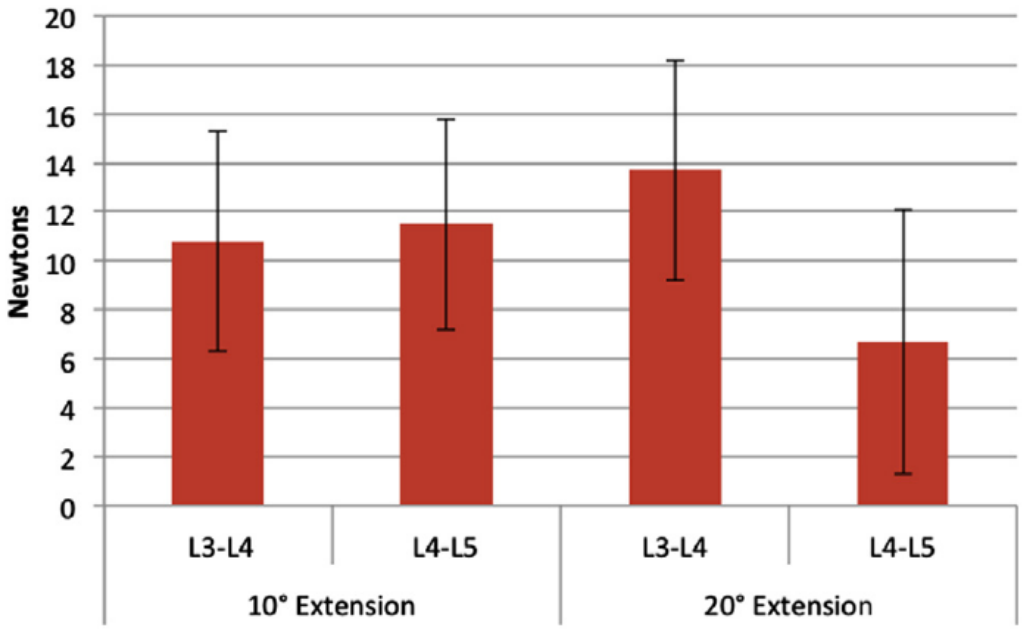

Figure 6 IFI mean facet joint differences

Table 2 Mean absolute differences and percent change in lumbar facet joint load between native IFS and simulated IFI

Facet Joint	L3-4		L4-5	
Degrees of Hip Extension	10°	20°	10°	20°
Facet loads with native IFS (SEM)	41.88 N (11.78)	49.89 N (14.00)	24.03 N (7.89)	34.93 N (9.84)
Facet loads after IFI simulation (SEM)	52.7 N (13.36)	63.61 N (16.10)	35.52 (8.83)	41.61 (8.54)
Mean absolute difference (SEM)	10.82 N (4.53)	13.71 N (4.53)	11.49 N (4.33)	6.67 N (5.43)
95% confidence interval	0.84-20.8	3.7-23.6	1.8-21.1	−5.2 to 18.6
P value	.036	.012	.024	.245
Mean percentage change	+28.16%	+32.01%	+31.00%	+32.07%

IFI, ischiofemoral impingement; IFS, ischiofemoral space; SEM, standard error of the mean.

2.4 Discussion

In the current study, IFI increased L3-L4 and L4-L5 facet joint loads by an average of 30.81% as compared with native conditions during hip extension. The mean difference of the absolute values was statistically significant for facet joint of L3-L4 at 10° and 20° of hip extension, and L4-L5 at 10° of hip extension. Although no statistical significant difference was detected for L4-L5 at 20° of hip extension because of the high force variability found in this joint, a similar pattern on absolute values and a similar percentage change (+32.07%) was found.

In the United States, more than 1.5 million lumbar magnetic resonance imaging studies are performed every year, with 300,000 reporting nerve root compression and only 200,000 patients obtaining relief from discectomies and other surgeries directed at relieving pressure on the spinal roots.[2] Physicians who treat patients with spinal-related problems should recognize that other Orthopaedic diagnoses involving the hip or lower limb are present in approximately 86% of the cases.

Hip-spine syndrome was first described more than 30 years ago,[3] and to date there are no publications describing the biomechanical effects of limited hip range of motion on lumbar spine loading. The hip-spine effect requires further definition and a quantitative model to study the effects of diminished terminal hip extension. This biomechanical model will allow for new studies, diagnostic, and therapeutic alternatives in patients with lower back pain who do not get relief after nonoperative or operative interventions for presumed lumbar spine pathology.[20]

As previous reports concluded that limitation on hip motion was the reason for lumbar spine symptoms, IFI is a valuable model to explain the hip-spine effect. An abnormal contact between the lateral aspect of the ischium and the lesser trochanter of the femur produces

limitation of terminal hip extension,[21] thus generating secondary pelvic rotation, hyperlordosis, and face joint overload.

Prior case reports and series have described concomitant lumbar disturbances in patients with hip pathologies; however, there are very few studies proving a causation pattern. Matsuyama et al.[6] evaluated the sagittal balance in patients with bilateral congenital hip dislocations and found that the most common clinical symptom was low back pain due to hyperlordosis.

A recent biomechanical study supporting the clinical finding that pelvic obliquity may play a role in increasing loads on spinal tissues, particularly the facet joints, was presorted by Popovich et al.[22] A hypercurved lumbar lordosis increases contact forces mainly on the posterior elements (facet joints, spinous process). The distribution of the forces generates a resultant sliding force, increasing the load on the facet joint and decreasing the load on the anterior intervertebral disc. Chronic mechanical stress may play a role in degenerative spine progression and pain.[23]

Although the current study proves the relation between IFI and lumbar spine overload by limiting the terminal hip extension, reports of patients getting relief of lower back pain after treating hip conditions have been published by Lejkowski and Poulsen[8] after physical therapy, Redmond et al.[7] after hip arthroscopy, and Ben-Galim et al.[4] after total hip replacement.

Other hip problems such as flexion contracture, posterior acetabular overcoverage, and femoral retroversion may have similar effects on the lumbar spine. To define hip or spine pathology, a comprehensive physical examination assessing the osseous, capsulolabral, ligamentous, musculotendinous, neurovascular, and especially the kinematic chain is crucial to the care of the patient with hip or spine pain.

This study has several strengths. First, full cadavers were used for testing, allowing for an approximation of real biomechanical conditions. Second, facet joint force was measured with a previously validated and published method. Finally, this study showed reproducibility in the small SDs and used previous techniques to show a significant change in loading.

2.5 Limitations

There are limitations to the present study. First, dynamic muscular action contributing to spine stability cannot be tested in cadavers. Muscles offer stability to the spine and influence forces on facet joints. Second, ligament creep, defined as the time-dependent elongation of a ligament when subjected to a constant stress, can affect the measurements of the last repetitions in every test condition. Third, tests were performed in a lateral position without reproducing the weight-bearing forces, which also influences the forces on the lumbar spine and posterior elements. Fourth, lesser trochanter size after IFI simulation was not calculated. Fifth, although using cadavers is a strength because it includes the spine, the remainder of the lower extremity could create a margin of error in measuring the amount of hip extension. Finally, L5-S1 facet joints were not tested because of the lack of previous validation for this joint with the measurement method used in this study. In addition, in all cadavers, the L5-S1 joints were consistently stiff and tight and did not all for sensor placement.

2.6 Conclusion

Limited terminal hip extension due to simulated IFI significantly increased L3-L4 and L4-L5 lumbar facet joint loading when compared with non-IFI native hips.

Chapter 3

Aim 2: The effect of cam-type femoroacetabular impingement on intervertebral disk loading

3.1 Introduction

Anterior hip impingement, specifically Femoroacetabular Impingement (FAI), is increasingly observed in the population. First described in 2003 by Ganz et al., FAI is characterized by either cam impingement of pincer impingement, or a combination of both.[10] Both types of FAI are abnormalities of the proximal femur (cam) or acetabulum (pincer). Cam impingement is an increased in bone volume in the femoral head-neck junction, whereas Pincer impingement is characterized by overcoverage of the acetabulum.[24] The repercussions of FAI impingement include an "outside-in" abrasion of acetabular cartilage, and labral tearing and occurs generally during hip flexion, internal rotation, and adduction.[24] Prolonged impairments affects activities of daily living.

Recent investigations into the hip and spine complex has revealed significant biomechanical interactions. Gómez-Hoyos et al. first reported on the deleterious effect of ischiofemoral impingement on lumbar facet loading. A significantly significant increase was observed in lumbar facet joint loading during hip extension to 20 degrees. On average, the facet joint loading increased 30.81% with simulated Ischiofemoral Impingement, when compared to native hips in hip extension.[25] A subsequent investigation assessed the relationship between abnormal femoral version and the Iliofemoral ligament on lumbar facet joint loading. Results from this study showed a decrease in loading with simulated decreased femoral version, and a further decrease with the Iliofemoral ligament released. Although the results were contrary to the

authors' initial hypothesis, an important biomechanical relationship was displayed. A complex biomechanical effect is transferred to the lumbar spine section as a result of abnormal hip pathology.

The advanced knowledge of the kinematic chain interaction between the hip joint and spine is critical for proper treatment, both conservative and surgical. The previous two studies described are direct translational problems commonly observed in Orthopaedic practice. The hip pathologies assessed were biomechanically tested during hip extension, as this position has most commonly been observed clinically and provides the strongest disturbance to the kinematic chain. The effect of flexion has not been examined. There is a multitude of hip and spine pathologies that require assessment in order to gain a complete understanding of this intricate complex. The purpose of the proposed study is to develop a flexion hip-spine model of anterior hip impingement to observe the loading in intervertebral disk space during hip flexion. The significance of this study will allow clinicians and therapists to obtain an advanced knowledge of hip-spine complex biomechanics. The hypothesis states that a significant increase in intervertebral disk loading will occur in the presence of simulated anterior hip impingement during hip flexion.

3.2 Materials & Methods

3.2.1 Specimens

Ten hips from five fresh-frozen T12-toe cadaveric specimens were utilized to assess the impact of cam-type impingement on the lumbar spine during dynamic hip flexion. All specimens were male with an average age of 56.9 years. The registered causes of death were not associated with

orthopaedic issues and did not affect the musculotendinous structures of the hip, pelvis, or lumbar spine. Each specimen underwent a physical examination of the hip, pelvis, and lumbar spine by a fellowship trained Orthopaedic surgeon (JGH) to exclude any pathology that would limit hip flexion and internal rotation or impede physiologic transduction to the pelvis and lumbar spine.

Demographic exclusion criteria included BMI greater than 30, age greater than 75. Physiological exclusions preventing full range of hip motion comprised arthritis, osteoporotic or metastatic lesions, gross cam deformity, coxa profunda or protrusion, and abnormal McKibben's index greater than 60 or less than 20.[26] Additional exclusions included previous hip or spine surgeries and abnormal sacral slope.

3.2.2 CT Imaging Evaluation

All cadaveric specimens underwent axial, coronal, and sagittal CT scan (General Electric Medical Systems LightSpeed RT16 XTRA, GE Healthcare, Buckinghamshire, United Kingdom) sequences of the lower limbs, pelvis, and lumbar spine prior to biomechanical testing. Anatomical evaluation of CT sequences was performed in GE MediaViewer 5 (GE Healthcare, Buckinghamshire, United Kingdom). The LCA and alpha angle were measured for to rule out native cam-type impingement. Additional hip measures included femoral neck version, acetabular version, femoral neck-shaft angle, and ischiofemoral space. Spine measures included L4-L5 intervertebral angle, sacral slope, and lumbar spine Cobb angles on the frontal and sagittal planes.

3.2.3 Intradiscal Loading Measurement

The L3-L4, L4-L5, L5-S1 segments were accessed through a direct anterior approach. Force transduction in the intervertebral disk was measured with a FlexiForce® force sensor (Tekscan, South Boston, MA, USA). The force sensor was inserted directly into the anteromedial section of the lumbar disk segments. The lumbar spine was accessed anteriorly to expose the spine segments. An incision was created with a size 15 scalpel to match the size of the sensor used. The force sensor was positioned to measure loading in the annulus fibrosus section of the intervertebral disk. (Figure 7)

Figure 7 FAI IVD sensor placement

3.2.4 Anterior Hip Impingement Model

A FAI Cam-type morphology was created using a 1.5 inch wooden knob. An osteotomy was performed to resect the anterolateral portion of the greater trochanter. The knob was placed at the osteotomy site and a screw was placed directly into the femoral neck, simulating a Cam deformity. The anterior hip impingement simulation is based on a previously published method by Birmingham et al.[11] (Figure 8)

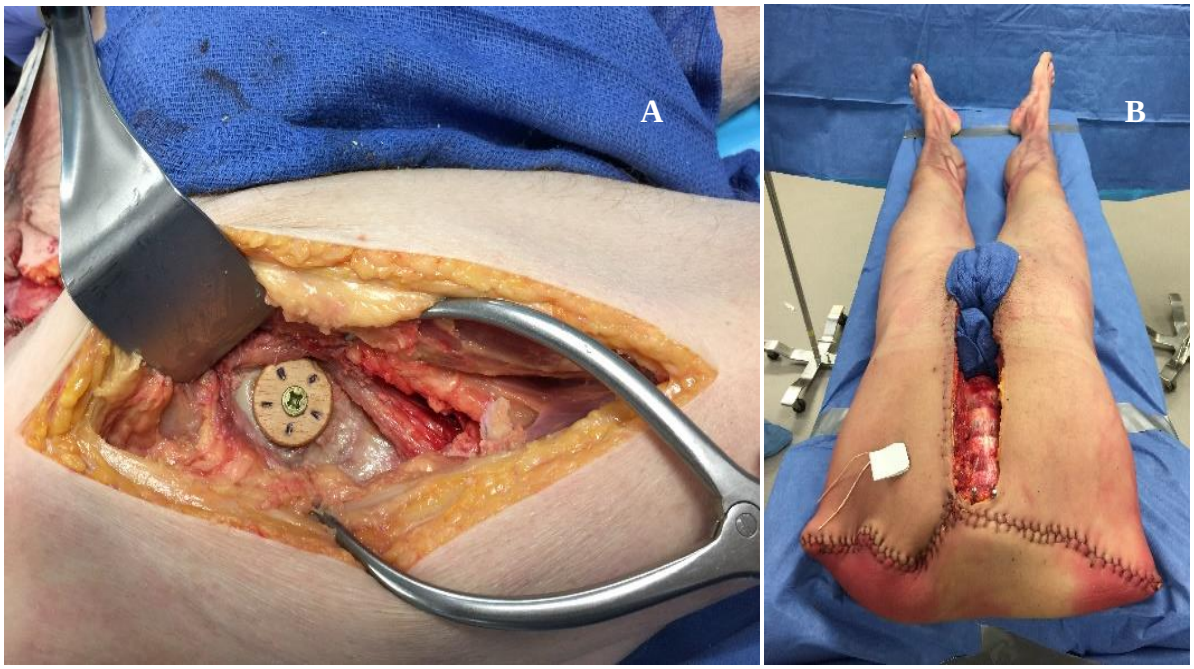

Figure 8 FAI experiment preparation

A. Cam-type FAI simulation. B. Cadaver placement on dissection table

3.2.5 Measurements and Hip Positions

The cadaveric specimen was placed in a supine position on a dissection table. (Figure 8) No attachments or supports were place distal to the pelvis to permit freedom of motion in the hip joint. Two Schanz pins were inserted through the L1 vertebral segment to prevent movement and axial rotation during hip flexion movements.

One examiner conducted the hip flexion and internal rotation movements. All motion began in a neutral hip abduction and external/internal rotation state. The following hip flexion positions were tested: 90 degrees, 90 degrees + internal rotation (IR), 120 degrees, 120 degrees + IR, and impingement test. Impingement test was classified as maximal hip flexion and internal rotation. Each position was repeated for three cycles. All examiners except for the intradiscal pressure sensor operator were blinded to results.

3.2.6 Statistical Analysis

Raw sensor data for the L3-L4, L4-L5, and L5-S1 IVD segments was compiled in Microsoft Excel (Microsoft, Redmond, WA). Subsequent statistical analysis was performed in SAS version 9.4 (SAS Institute, Cary, NC, USA). A three-way repeated measures ANOVA with all within-subject factors was used to observe significant effects between FAI, hip flexion, and IVD sensor location. Alpha was set to 0.05.

3.3 Results

Twelve cadaveric hip specimens (6 cadavers) were considered for this investigation. One cadaver was ruled out due to advanced tissue deterioration upon visual inspection. Ten cadaveric

hips from five cadaveric specimens were utilized to assess the effect of simulated FAI on the lumbar IVD during hip flexion. The cadaveric donors were all male with an average age of 56.9 years (range: 36 – 73; SD: ±12.1). The anatomic hip measurements obtained from CT imaging included femoral neck version (17.9° ±14.15), acetabular version (19.66° ±7.76), femoral neck shaft angle (131.5° ±4.04), and ischiofemoral space (23.7 mm ±9.32). Spine measurements included L4-L5 intervertebral angle (11.6° ±2.16), sacral slope (47.1° ±7.85), and pelvic incidence (56.7° ±15.93). (Table 3)

Table 3 FAI Cadaver demographics

	AVG	**SD**
Age (yrs)	56.9	12.1
FNV (°)	17.90	14.15
AV (°)	19.66	7.76
FNSA (°)	131.5	4.04
IFS (mm)	23.7	9.32
L4-L5 Intervertebral Angle (°)	11.6	2.16
Sacral Slope (°)	47.1	7.85
PI (°)	56.7	15.93

Average loading in the native L3-L4 IVD for 90° and 90° + IR hip flexion was measured to be 34.29 N ±37.34 and 44.18 N ±51.36. Loading increased during hip flexion to 120° (47.38 N ±64.73) and 120° + IR (58.68 N ±84.16). Impingement test, considered to be maximal hip flexion and internal rotation, was measured to be 55.8 N ±70.4). Simulated FAI increased loading in the L3-L4 IVD. Average loading in the for the FAI case for 90° and 90° + IR hip

flexion was measured to be 38.12 N ±55.65 and 46.89 N ±60.75. Average measured loading for 120° was 71.06 N ±101.75 and 120° + IR was 65.24 N ±89.52. The impingement test slightly increased L3-L4 IVD loading and was measured to be 56.3 N ±72.27. (Figure 9)

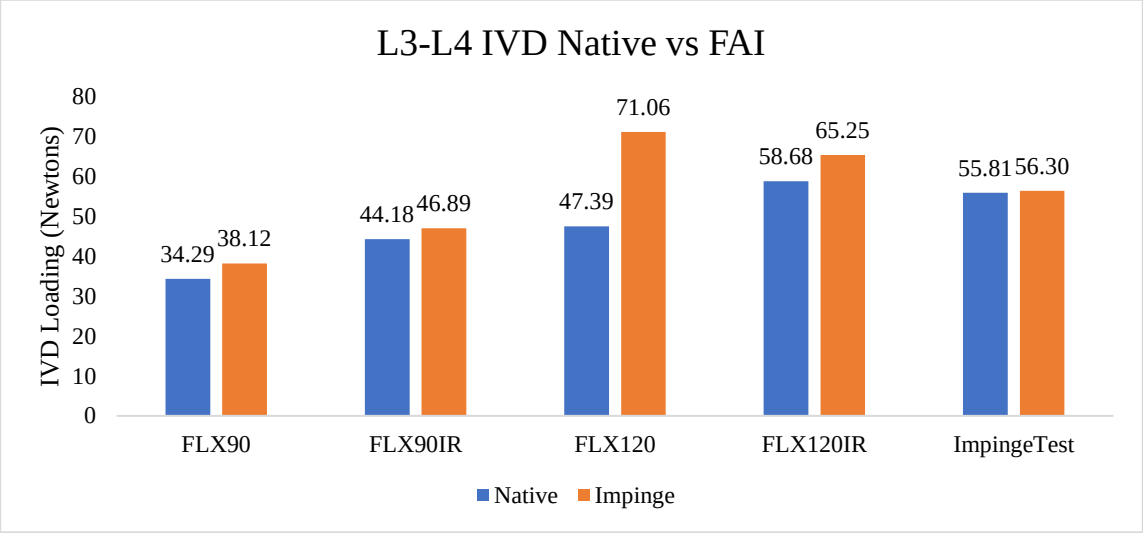

Figure 9 FAI L3-L4 Loading

Average loading in the native L4-L5 IVD for 90° and 90° + IR hip flexion was measured to be 57.4 N ±61.36 and 90.94 N ±104.59. Loading increased during hip flexion to 120° (109.66 N ±126.24) and 120° + IR (97.07 N ±128.99). Impingement test, considered to be maximal hip flexion and internal rotation, was measured to be 97.98 N ±118.49). Simulated FAI increased loading in the L4-L5 IVD. Average loading in the for the FAI case for 90° and 90° + IR hip flexion was measured to be 79.05 N ±100.02 and 89.67 N ±96.99. Average measured loading for 120° was 140.45 N ±157.88 and 120° + IR was 146.32 N ±159.42. The impingement test slightly increased L4-L5 IVD loading and was measured to be 114.97 N ±128.64. (Figure 10)

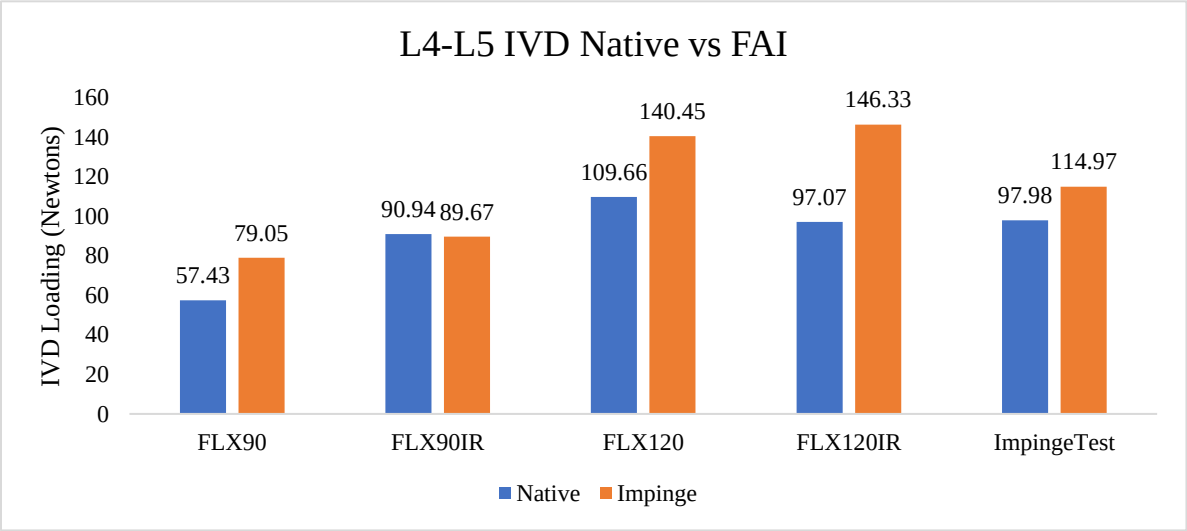

Figure 10 FAI L4-L5 IVD Loading

Average loading in the native L5-S1 IVD for 90° and 90° + IR hip flexion was measured to be 59.82 N ±57.12 and 71.12 N ±69.68. Loading increased during hip flexion to 120° (131.76 N ±128.5) and 120° + IR (129.72 N ±123.03). Impingement test, considered to be maximal hip flexion and internal rotation, was measured to be 132.67 N ±131.75). Simulated FAI increased loading in the L5-S1 IVD. Average loading in the for the FAI case for 90° and 90° + IR hip flexion was measured to be 90.74 N ±92.64 and 87.26 N ±90.57. Average measured loading for 120° was 162.78 N ±159.97 and 120° + IR was 144.15 N ±131.97. The impingement test slightly increased L5-S1 IVD loading and was measured to be 149.97 N ±147.64. (Figure 11)

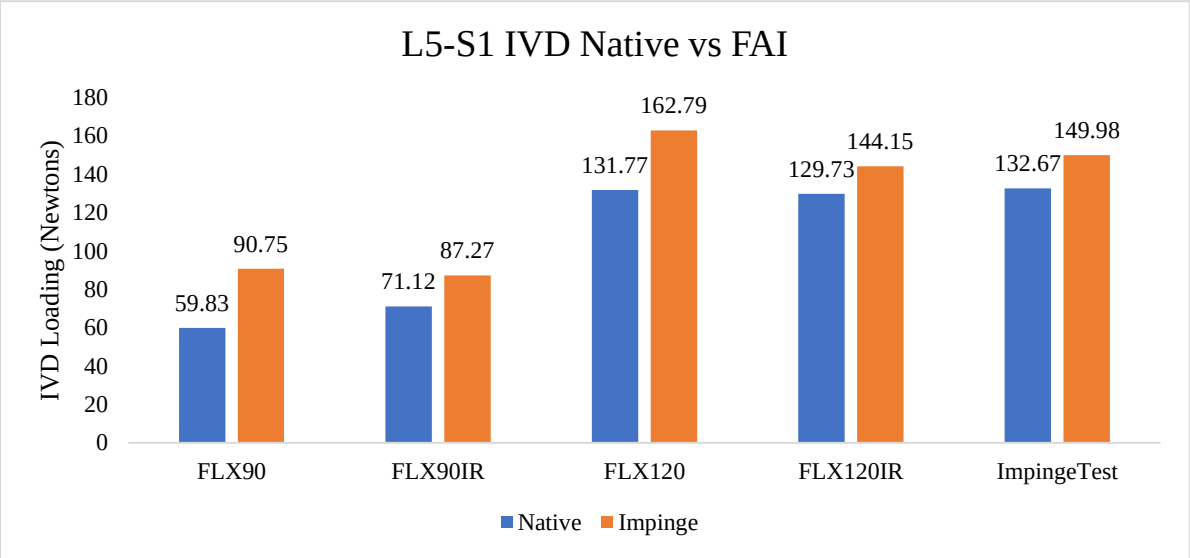

Figure 11 FAI L5-S1 IVD loading

A three-way repeated measures ANOVA with all within-subject factors was utilized to observe significant effects of simulated FAI compared to a native state during hip flexion and internal rotation. A significant effect was observed when comparing mean IVD loading between native (80.98 N ±101.46) and simulated FAI conditions (98.87 N ±121.53) ($p<0.0001$). Additionally, when comparing IVD location the L4-L5 and L5-S1 segments were significantly larger compared to the L3-L4 IVD segment ($p<0.0001$). The mean IVD loading during hip flexion to 90° and 90°+IR were observed to be significantly lower compared to the mean IVD loading in the other hip flexion and internal rotation positions tested.

In multivariable analyses, no significant association between impingement status and IVD pressure ($p=0.06$) was observed. However, location of sensor ($p=0.0004$) and hip flexion angles ($p=0.01$) are significantly associated with IVD pressure. No significant interactions between simulated FAI and location of sensor or hip-flexion angle with IVD pressure were observed. However, significant interaction between location of sensor and hip-flexion angles

suggest that sensor location within the IVD segments at a particular hip-flexion angle significantly influenced IVD pressure.

3.4 Discussion

Cam-type femoroacetabular impingement is classified as one of the several dynamic impingements occurring between the femoral neck and acetabulum.[27] The clinical presentation and surgical treatment outcomes have been of great interest to the sports medicine and hip preservation community. The current study aims to further the understanding of dynamic hip impingement by investigating the effect of cam-type FAI on the lumbar spine IVD. The kinematic chain occurrence resulting from dynamic impingement quantifies the biomechanical relationship between the pathological hip and the spine.

The resultant data from this investigation show a substantial increase in measured IVD loading in a simulated FAI condition during hip flexion and internal rotation, when compared to a non-impinged native hip state. All cases display an increase of IVD loading between native and cam-type FAI hip states, with the exception of FLX90 +IR in the L4-L5 IVD. In this case there was a miniscule decrease. Although the increased loading was observed, no significant effects were found when comparing individual hip flexion states. This is due to the large variance associated with cadaveric specimens. This investigation was aimed toward understanding a global kinematic chain effect between the hip and lumbar spine. Exclusion criteria for cadaveric specimens allowed the investigators to obtain a reasonable number of samples, however stringent controls are difficult in these large-scale cadaveric studies. The three-way ANOVA suggests a significant increase in loading associated to the L4-L5 and L5-S1 IVD compared to the L3-L4

IVD. Additionally, the hip flexion of 90° and 90°+IR were significantly lower. This is consistent with clinical presentations of FAI due to the impingement not being as impactful in this region.

The clinical repercussions related to cam-type FAI have been studied extensively. Conditions including osteoarthritis, cartilage delamination and labral tears are characteristic factors resulting from repetitive contact between the increased bone volume of the femoral head-neck junction and acetabulum. A recent investigation by Ng et al. evaluated the torsional loading before and after cam-type FAI surgery in a cadaveric model.[28] The resultant data suggest a cam-type pathology contributes between 21% to 27% of an intact hip resistance to torsional load during hip flexion and internal rotation. Therefore, the removal of the cam-type pathology is essential to decrease the loading placed on the chondrolabral junction. The decrease in lumbar IVD loading associated with non-cam-type impingement hips can also be attributed to the reduction of torsional load resistance.

Recent investigations regarding anterior hip impingement and pelvic consequences have been conducted. Birmingham et al. introduced a simulated cam impingement to assess the impact of rotational motion at the pubic symphysis.[11] Resultant data concluded cam impingement contributing to pubic symphysis rotation, an approximate 35% increase, after impingement occurs. Although pubic symphysis motion is common, premature contact as a result of abnormal bony hip parameters including cam impingement or decreased femoral version result in pathologic motion, especially during sports activity. Lamontagne et al. studied pelvic motion during maximal squat in subjects with cam impingement.[24] No differences in hip motion during the squat motion were observed in subjects with FAI compared to the control group, however the FAI group on average was not able to squat as low. A significant finding observed was a decrease in sagittal pelvic range of motion in the FAI group compared to the control group. The

authors propose premature contact between the femur and acetabulum may occur with reduced sagittal pitch, however femoral torsion parameters were not controlled. Similar findings regarding no significant difference in maximal squat have been confirmed by Diamond et al.[29,30]

A critical factor within the hip-spine-pelvis core pathomechanics is sagittal plane imbalance. The impingements and bony abnormalities addressed affecting the mechanotransduction of load through the spine do so by influencing pelvic planes. Deviations in pelvic position alter spinal alignment.[23] The normal curvature of the lumbar spine allows for load to be uniformly distributed through the length of the spine. The gait studies by Diamond et al.[29,30] and Lamontagne[24] reported no significant differences in hip biomechanics during squatting movements, however both authors theorize limited sagittal plane motion as a influential factor in patients with symptomatic FAI. A decrease in sagittal plane range of motion is a common factor in symptomatic FAI patients.[30–32] Additionally, patients with symptomatic FAI pathology were shown to have 13° less spinal flexion.[33] The decrease in sagittal plane motion and spinal flexion supports the findings of the current study. Absence of compensatory normal spinal motion can increase IVD loading. Operative correction of FAI pathology can help to restore sagittal plane range of motion as presented by Rylander et al. during which an overall increase of 3.1° sagittal plane range of motion was observed.

3.5 Limitations

The presented study of simulated cam-type FAI does have limitations. Hip flexion movement to 90 and 120 degrees was performed manually. Standardizing this procedure with available robotic devices can help to achieve accurate data. The cadaveric specimen was placed in the supine position on the dissection table. The supine position negates the effect of weight-bearing forces

typically observed, and this factor can contribute to overall lumbopelvic mechanics. A final limitation is this investigation did not assess the effect of pincer impingement. Pincer impingement can also affect the mechanics during hip flexion.

3.6 Conclusion

The cadaveric model of cam-type FAI increased L3, L4, and L5 IVD loading during hip flexion, compared to a non-impingement native state. Deep hip flexion to 120 degrees and 120+IR resulted in the largest lumbar IVD loading.

Chapter 4

Aim 3: The effect of increased and decreased femoral anteversion on the lumbar spine

4A Increased and decreased femoral anteversion will be simulated in cadaveric specimens and facet joint loading will be measured during hip extension to 10° and 20° with normal hip abduction.

4A.1 Introduction

Low back pain and its related disabilities are major societal problems. Eighty percent of all people experience low back pain (LBP) at some point in their lives.[1] Separating hip and spine pain is difficult and lower back complaints are the most frequent reason to seek Orthopaedics or neurosurgery consultation. LBP is also the second leading reason for physician visits.[1] The majority of patients show no abnormalities on magnetic resonance imaging and do not achieve pain relief from procedures directed at alleviating pressure on the spinal roots.[2]

A pathologic sequence of abnormal hip range of motion (e.g., limited hip extension due to an abnormal version or hip flexion contracture), forward pelvic rotation, and lumbar hyperlordosis could generate lumbar facet joint changes.[3] Abnormal hip range of motion can affect the iliofemoral ligament discrepancies, as this ligament could limit hip extension. As a result of interrelated axial skeleton adaptions low back pain symptoms could be produced in patients with any condition involving limited hip extension.

Offierski[3] described the term "Hip-Spine Syndrome" in 1983 as a probable cause of lumbar problems generating or worsening from hip abnormalities. No biomechanical study was performed to validate the hypothesis. In 2016 Gomez-Hoyos et al.[25] devised a cadaveric model demonstrating a relationship between hip pathology and lumbar spine kinematics, more specifically the interaction between ischiofemoral impingement and lumbar spine loading.

The purpose of this study is to assess the effect of femoral version and the iliofemoral ligament on lumbar facet joint load during hip extension. The hypothesis states change in femoral version, as well as iliofemoral ligament function affects L3-4 and L4-5 facet joint loads in cadaveric specimens in terminal hip extension.

4A.2 Materials & Methods

4A.2.1 Specimens

Sixteen fresh-frozen hip specimens from T1-to-toes cadavers (no arms) were utilized. The registered causes of death were unrelated and did not affect the integrity of the hip, pelvis and/or spine. The donors included four males and four females who were 65.3 years of age on average.

Specimens were excluded based on visual gross morphologic deformity or pathology (e.g., scoliosis, osteoporotic or metastatic lesions, previous surgeries or trauma, abnormal lumbar lordosis or sacral slope) and computed tomography scan with evidence of any major degenerative disease (osteoporosis, osteoarthritis, etc.). Specimens with soft tissue contracture (positive Thomas test) around the hip were excluded. An orthopaedic surgeon assessed all the specimens.

4A.2.2 Pre-measurement Imaging Evaluation

Axial, coronal, and sagittal computed tomography scan sequences (General Electric Medical Systems LightSpeed RT16 XTRA, GE Healthcare, Buckinghamshire, United Kingdom) of the spine, pelvis, and lower limbs were performed on all cadavers prior to biomechanical testing. The feet were taped to fix the lower extremity in a functional walking position, with neutral

abduction in order to simulate real gait conditions and to maintain consistency during imaging assessment of cadaveric specimens, as in prior validated study.

CT images were analyzed in GE MediaViewer 5 (GE Healthcare, Buckinghamshire, United Kingdom) to calculate the native (original) femoral version and McKibbin's index of the specimens. Hip measures included femoral neck version, acetabular version, femoral neck-shaft angle, ischiofemoral space, and tibial torsion. Spine measurements were intervertebral L4-L5 angle, sacral slope, and lumbar spine Cobb angles on the frontal and sagittal planes. Additionally, leg length (from the center of the femoral head to the center of the tibiotalar joint), and knee varus/valgus angle were measured.

4A.2.3 Specimen Set up

Cadavers were positioned in lateral decubitus on a dissection table. Two fixated boards (2 feet by 1 feet) were positioned anterior to the chest and posterior to the lumbar spine (distal border of the board proximal to L2) to stabilize the upper torso and simulate the normal sagittal balance in an upright posture. The examined leg was placed on the testing frame with the hip joint in a neutral position and the tibiotalar and subtalar joints locked at 90 degrees with a custom designed foot bracket. The knee was transfixed with two Steinmann pins in 0 degrees extension simulating terminal hip extension during gait. The contralateral leg, locked in the same manner, was placed on the dissection table in 20 degrees of hip flexion and fixated with a Schanz pin (Stryker, Kalamazoo, Michigan, USA) simulating a normal gait position.

4A.2.4 Surgical Approach and Measurement Methods

A posterior approach to the lumbar spine was performed down the middle of the back through a 20 cm to 25 cm incision. The fat and lumbodorsal fascia to the spinous process was dissected

preserving the interspinous ligament. Paraspinal muscles were detached sub-periostally and dissected down to the spinous process and lamina to the facet joint. The L3-L4 and L4-L5 ipsilateral facet joint capsules were carefully incised about 10 mm, allowing for placement of an ultrasensitive piezoresistive force sensor (FlexiForce B-201; Tekscan, Inc., South Boston, MA, USA). The facet joint capsule was not resected in order to avoid considerable disturbances in facets anatomy or biomechanics. Direct visualization was used as a qualitative indication of sensor placement and was inspected after each testing condition. New sensors were used for every specimen and individually calibrated for both the left and right side to convert sensor saturation to Newtons.

4A.2.5 Increased and Decreased Femoral Anteversion Model

A transverse cut through the midshaft femur was performed using a 19 mm cut edge oscillating bone saw (Stryker, Kalamazoo, Michigan, USA). The osteotomy was done prior to any experiment to ensure consistency of measurements, both before and after de-rotational osteotomy. The osteotomy was held in place with a lateral external fixator including four Schanz screws, two 8-mm connecting rods and eight pin-to-rod couplings (Stryker, Kalamazoo, Michigan, USA). After testing for native rotation parameters, the external fixator was loosened and the femur (distal to the osteotomy) was rotated as needed to get +30 degrees of femoral neck version with the foot at to 0° rotation. The same procedure was performed again in each specimen in order to get -10 degrees of femoral version. (Figure 12)

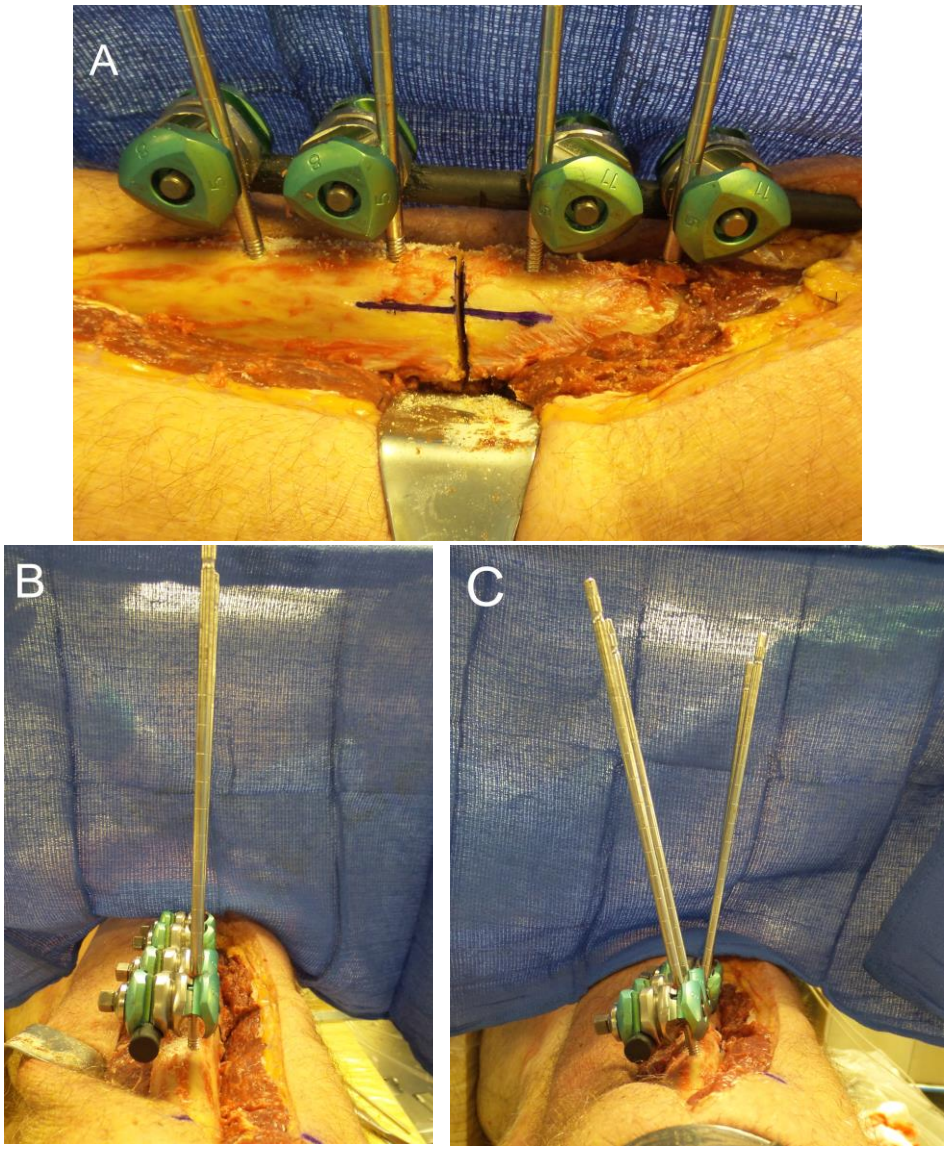

Figure 12 Femoral Version simulation

4A.2.6 Iliofemoral Ligament Release

After testing for native conditions and abnormal femoral neck version, an anterior approach to the hip was performed in order to expose the anterior capsule. The medial and lateral arms of the iliofemoral ligament were identified and resected in the mid aspect of the ligament.

4A.2.7 Measurements and Hip Positions

A PVC frame was built to provide support to the cadaver leg in neutral abduction during the experiment. Prior to all experiments, a 0° and 20° extension point was marked on the frame based on the center axis of the hip joint. To permit freedom of motion in the hip joint, no attachments were used during position manipulation.

The leg was moved in cycles from neutral position to the intended extension position for each testing condition by a trained physical therapist. Every cycle was performed starting in neutral abduction and extended at a speed of 10-degrees per second. The leg was held for 10 seconds at the starting and final position of each cycle to indicate start/end of experiment, and the timing was noted for data analysis. Every cycle was repeated five times by the same examiner for all experiments. All examiners, except for the piezoresistive force sensor operator, were blinded to results. The methods are based upon a previously validated protocol.

4A.2.8 Statistical Analysis

Microsoft Excel (Microsoft, Redmond, USA) was used to compile raw data in addition to calculating the percent change before and after experiments for femoral version with and without the ILFL intact. Statistical analysis was performed using SPSS (V) (SPSS, Inc., Chicago, Illinois). A two-way mixed ANOVA model was fitted to assess impact of femoral version effects

and hip extension effects on lumbar facet joint loading. A square root transformation was applied due to non-normality of the facet joint loading data. Alpha was set at 0.05.

Percentage change was calculated considering the difference between a native condition and a simulated one in each specimen. These calculations were supported by the fact that a high variation was found in native facet loads between specimens. Thus, a change from 10 newtons to 20 newtons meaning 200% percentage change should be equivalent to a change between 5 newtons and 10 newtons for another specimen.

4A.3 Results

Fourteen hip specimens (from seven cadavers) were considered for this study. One specimen was not included for data analysis as it was used for pilot experiments.

Thirteen hips were included for final analysis (7 cadavers). The donors included four females and three males who were 65.3 years of age on average (range, 50 to 75, SD ±8.4) and body mass index was 25.8 kg/m^2 on average (range, 15 to 34.2, SD ±9.8).

Native femoral neck version, acetabular version and tibial torsion were recorded (7.7° SD ±8.8, 21.0 SD ±4.7, and 28.6 SD ±2.1). Native ischiofemoral space was 23.7 mm (SD ±9.8) on average. Imaging parameters for axial, coronal and sagittal planes are shown in Table 4.

Table 4 Femoral Version demographic and imaging characteristics

Parameter (units)	Mean	Minimum	Maximum	Standard deviation
Age (years)	65.3	50.0	75.0	8.4
Body Mass Index (kg/m^2)	25.8	15.0	34.2	9.8
Leg length (cm)	79.6	72.4	88.3	5.3
Femoral neck/shaft angle (°)	131.0	122.0	140.0	5.2
Femoral neck version (°)	7.7	-4.3	22.3	8.8
Acetabular version (°)	21.0	11.0	27.0	4.7
McKibbin Index (°)	28.8	11.9	43.6	10.4
Native ischiofemoral space (mm)	23.7	11.6	43.2	9.8
Coronal Cobb angle (°)	1.3	0.5	2.6	0.7
Sagittal Cobb angle (°)	32.9	28.7	40.0	4.0
Sagittal L4-5 intervertebral angle (°)	12.0	8.7	13.9	1.7
Sacral slope (°)	40.8	34.0	47.1	4.4
Knee valgus (°)	5.0	1.9	7.0	1.8

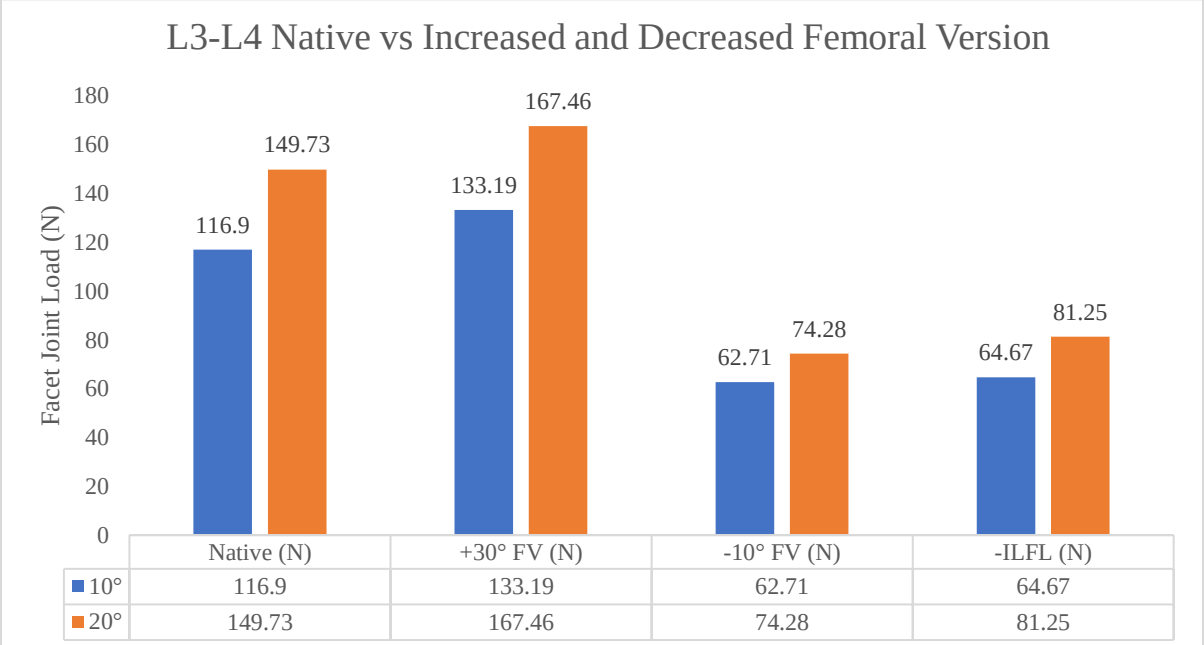

Figure 13 FV L3-L4 facet joint loading

The average baseline facet joint load in the native femoral version condition for L3-4 was 116.9 N (SD ±154.8) at 10 degrees of hip extension; the average facet joint load in the native femoral version condition was 149.7 N (SD ±170.9) at 20 degrees of hip extension. Increased femoral version (+30 degrees) increased L3-L4 facet joint loading in the presence of 10 degrees hip extension (133.19 N) and 20 degrees hip extension (167.46N). Decreased femoral version (-10 degrees) lowered L3-L4 facet joint loading during hip extension. Release of the iliofemoral ligament also reduced overall loading in the L3-L4 facet joints during hip extension. (Figure 13)

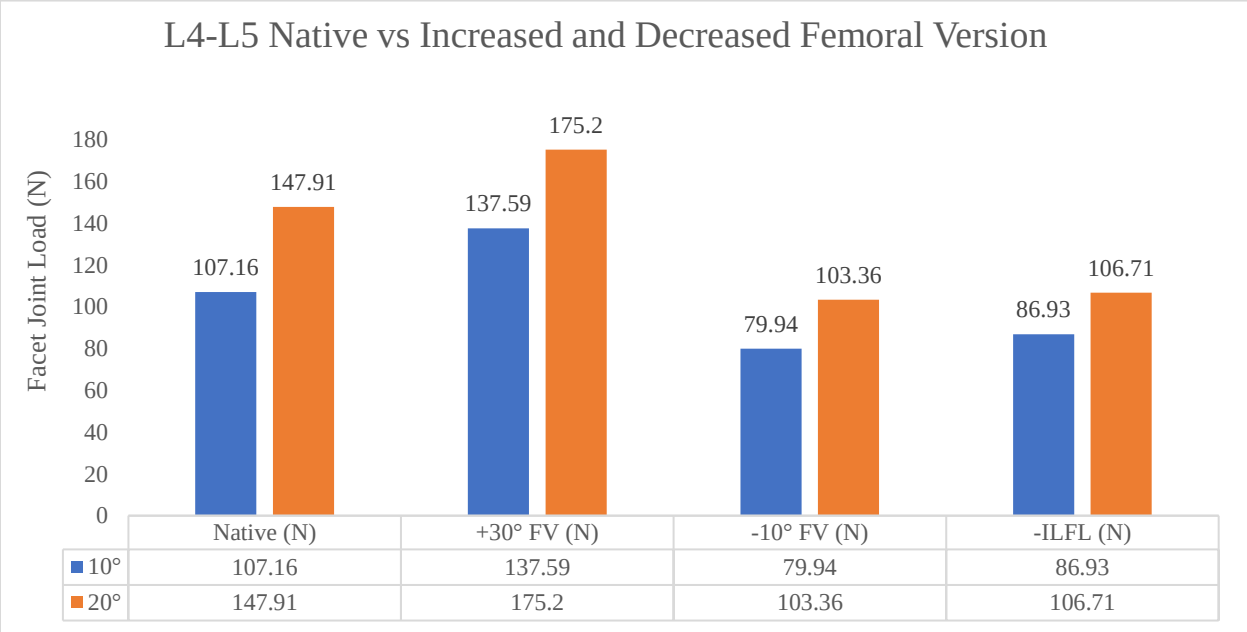

Figure 14 FV L4-L5 facet joint loading

L4-L5 native facet joint load was 107.1 N (SD ±138) for 10 degrees, and 147.9 N (SD ±159.6) for 20 degrees of hip extension. Similar to the L3-L4 facet joint loading, increased femoral version increased facet joint loading in the L4-L5 segments during 10- and 20-degrees

hip extension (137.59 N and 175.2 N). A decrease in facet joint loading was also observed for decreased femoral version during 10- and 20-degrees hip extension (74.94 N and 103.36 N) compared to native. (Figure 14)

Two-way ANOVA revealed significant effects. The increase in hip extension from 10 degrees to 20 degrees significantly increased facet joint loading ($p<0.001$). Decreased femoral version (-10 degrees) and released iliofemoral ligament resulted in a significantly lower facet joint loading compared to native states. A significant increase was observed for the increased femoral version condition (+30 degrees) in the L4-L5 facet joint ($p<0.04$), however was not observed in the L3-L4 facet joint.

Given the high variability of native facet joint loads between cadavers. Average of percentage change before and after every testing condition was recorded in order to calculate the effect of abnormal femoral version and iliofemoral ligament resection. (Table 5)

Table 5 Mean percentage change in lumbar facet joint loading and differences between simulated testing conditions

Facet joint	**L3-4**		**L4-5**	
Degrees of hip extension	**10 degrees**	**20 degrees**	**10 degrees**	**20 degrees**
Native vs. +30 FNV (SEM)	6.63% (13.06%)	1.67% (16.44%)	14.68% (13.16%)	6.00% (13.23%)
Native vs. -10 FNV (SEM)	-148.68% (62.68%)	-173.95% (74.98%)	-49.03 (21.82%)	-176% (76.20%)
Native vs. -10 FNV with iliofem cut (SEM)	-156.28% (65.45%)	-245.73 (165.88%)	-95.63% (38.67%)	-257% (144.48%)
Contribution of the iliofemoral ligament	7.61%	71.78%	46.6%	80.62%

An average lumbar facet joint underload of 51.65% on lumbar facet joints load was observed as a result of only the contribution of the iliofemoral ligament release, regardless of the femoral version. A complete report of percentage changes for different comparisons between testing conditions is presented in Table 5.

4A.4 Discussion

The results obtained from this cadaveric study confirm the proposed hypothesis that loading on the lumbar facet joints can be affected by femoral version and iliofemoral ligament contribution. Facet joint load during hip extension was significantly different ($p<0.013$) when increased femoral neck anteversion and femoral neck retroversion were compared. After releasing the iliofemoral ligament, lumbar facet loads decreased by 51.65% on average. These findings support the clinical notion that changes in hip motion may play a role in affecting loads on the lumbar facet joints.

The facet joints function to protect the intervertebral disk from excessive motions and load, including shear forces and injurious rotations. Tears of the annulus fibrous are resultant of large axial rotation. In the presence of the axial rotation, compression of contralateral facet joint protects intervertebral disk tissue from motion.[34] Results from the current study as well as previous experiments aimed to study the effect of hip extension on lumbar facet joint biomechanics show a direct relationship with abnormal femoral anatomy. The present experiment describes the effect of femoral version variations on the biomechanics of the lumbar facet joint.

The vector of the ground reaction force changes throughout the gait cycle. Heel strike (initial contact) drives the ground reaction force vector anterior to the hip joint. The

force vector is directed posteriorly as the gait cycle continues through the terminal swing phase.[35] The axial orientation of the femoral neck is closely related to the capsulolabral and musculotendinous structures of the hip and lumbar spine. The ground reaction force transmission through the hip joint may be interrupted by a change in orientation of the femoral head.

Rotatory alignment of the long axis of the femur to the hip is dictated by femoral version. Version of the femoral head, associated with inclination of the pelvis, makes it possible for flexion movements of the hip joint to be transposed into rotatory movements of the femoral head of the femur.[36] These rotatory movements of the femur depend largely in several factors such as muscle activity and kinetic direction, which is directly guided by the rotation and tilt of the pelvis and pelvic-femoral soft tissue.

Changes in facet joint load are a result of compensation in pelvic tilt. Limited hip extension generates sagittal balance compensations, thus impairing the backward step and causing a compensatory anterior tilt of the pelvis to align the limb with the ground in the stance phase. Changes in femoral neck version effect the sacral slope and may induce lumbar hyperlordosis which opposes forward flexion of the trunk.[37]

Decrease in facet joint motion was observed with releasing the medial and lateral arms of the iliofemoral ligament. The contribution of the iliofemoral ligament on the lumbar-pelvic-femoral connection, as acute changes in femoral version could lead to changes in capsular ligament tension and configuration, thus affecting lumbar facet joint loads. Simulated femoral neck retroversion could lead to loosening of the iliofemoral ligament and mimic a ligament release. This is even more expectable as the soft tissue is the actual connection between pelvis and hip. If the hip capsule were totally absent, for instance, femoral neck version would not affect pelvic obliquity during hip extension.

The pattern of hip capsule function is initial restriction of medial rotation, followed by extension, abduction, and finally lateral rotation.[38] From midstance to pre-swing the stance leg needs to medially rotate and extend. Capsuloligamentous and muscular restrictions to extension and medial rotation will force the lumbar spine to increasingly rotate contralaterally to compensate for hip restrictions and maintain normal stride length. Contralateral lumbar rotation will cause increased compressive forces over the ipsilateral impacted facet joint.

A recent systematic review about the hip-spine connection reported studies in patients with low back pain demonstrating limited hip range of motion. The patients routinely improved after surgical intervention for hip disease.[7] Internal rotation improvements are associated with arthroscopic decompression of cam deformity, then improving the internal hip rotation by fixing a cam-type in a patient with femoroacetabular impingement could explain the lower back pain relief in these cases.

New advances in sagittal analysis make it possible to define the intrinsic extension reserve within the global extension reserve of the spino-pelvic-femoral complex. This motion is essential for assessing intrinsic limited hip extension due to a number of causes.

The results obtained from this study again show the significant biomechanical link of the hip in relationship to the lumbar spine through both osseous and ligamentous contribution. Further studies assessing the incidence of lower back pain in patients with abnormal version and hip flexion contracture, as well as studies reporting clinical outcomes after addressing these problems should be conducted.

4A.5 Conclusion

Femoral version and iliofemoral ligament function release effects L3-4 and L4-5 facet loads as compared under the conditions of hip extension in cadaveric specimens.

4B Lumbo-pelvic gait changes will be monitored using gait analysis techniques in patients with decreased femoral version compared to normal patients, during a normal gait cycle.

4B.1 Introduction

The hip-spine relationship has been under recent scientific investigation due to anatomical proximity and complementary biomechanics. As a result, predictive factors for low back pain include: abnormal hip anatomy, preexisting hip pathologies, differences in hip range of motion, and muscle strength.[7,39–45] A biomechanical exploration of the relationships between variations in hip morphology and the lumbopelvic motion during gait would aid in the understanding of this complex area.

Femoral anteversion is the axial orientation of the femoral neck relative to the posterior condyle axis of the knee. Normal femoral anteversion is estimated to be anteriorly oriented in 10° for males and 20° for females.[46–49] Subjects with altered femoral anteversion tend to present with hip rotational misalignment related to hip and lower extremity gait abnormalities. In cases of decreased femoral anteversion (males<5° and females <10°), gait examination reveals an external foot progression angle due to an adaptation to centralize the femoral head.[46–49] The influence of decreased femoral anteversion on lower extremity alignment and early development of hip pathologies, such as osteoarthritis, has been of great interest in recent years.[50–54]

Disturbances at the level of the hip joint can affect the kinematics of the pelvis and the spine.[55–58] Decreased femoral anteversion requires rotational compensation by the lower extremities and may influence the pelvis and spine motion. To date, only torsional hip abnormalities as a result of neurologic and degenerative diseases affecting kinetics and kinematics of the hip and pelvis have been investigated.[59–62] The influences of decreased femoral version on the hip, pelvis, and lumbar spine biomechanics during gait are unknown.

The purpose of this study is to investigate the influence of decreased femoral anteversion on hip, spine, and pelvic motion during gait. The hypothesis states decreased femoral anteversion will affect spine and pelvic motion during gait.

4B.2 Materials & Methods

4B.2.1 Patient Selection

Following Institutional Review Board approval, 40 subjects were recruited from a center specializing in hip preservation and restoration surgery. A complete physical examination was completed that included ROM measures as described.[63] The inclusion criteria for the decreased femoral anteversion group (DFAG) were: positive Craig's test for decreased femoral version, internal rotation (IR) less than 8°, external rotation greater than 25°,[64] absence of hip conditions that limit terminal hip extension (flexion contracture, ischiofemoral impingement and coxa-profunda), [43] and a standardized MRI examination confirming the femoral anteversion as less than 5° degrees for males and less than 10° for females. Exclusion criteria were: hip conditions that limit terminal hip extension (flexion contracture, ischiofemoral impingement and coxa-

profunda), [43] any other orthopedic, or neurological disorders that could interfere with gait function.

4B.2.2 Subjects

The control group (CG) consisted of 20 volunteer subjects (14 male and 6 female) with a mean age of 32.98 (SD 11.61) who had confirmed normal femoral version (Craig's test) and normal hip range of motion, IR = 30.9 (SD 11.8) and ER = 26.4 (SD 10.4), [65] and no history of low back or hip pain. The decreased femoral version group (DFVG) consisted of 20 subjects (12 female and 8 male) with a mean age of 41.19 (SD 10.83). The mean femoral version of the DFVG was -1.65° (SD 5.36) (average males -3.14°; average females -1.08°). The complete demographic data are demonstrated in Table 6.

Table 6 Demographic characteristics of subjects

Group	**Femoral Version**	**Age (years)**	**Weight (Kg)**	**Height (m)**	**BMI**	**Gender (Female)**
DFVG (20)	-1.65° (SD 5.36)	41.19 (SD 10.83)	75.26 (SD 16.68)	1.68 (SD 0.10)	26.49 (SD 4.73)	12 (60.0%)
CG (20)	N/a	32.98 (SD 11.61)	74.99 (SD 13.50)	1.77 (SD 0.11)	23.91 (SD 3.37)	6 (30.0%)
P-Value	N/a	**0.026**	0.956	**0.012**	0.054	

4B.2.3 Gait Analysis

Kinematic and Temporal-Spatial data were collected at 100 Hz with use of a twelve-camera digital Vicon motion capture system (Vicon, Denver, Colorado). Visual 3D (C-Motion, Bethesda, Maryland) was used for data processing. Retro-reflective markers were placed bilaterally on the anterior superior iliac spine and the posterior superior iliac spine, laterally on the femur, on the lateral epicondyle of the knee, laterally on the tibia, on the lateral malleolus, on the head of the second metatarsal, and on the posterior aspect of the calcaneus at

the same height as the marker on the second metatarsal head. (Figure 15) A custom surface spinal triad marker was placed at the T12, L3 and L5 segments. [66,67] (Figure 15) Subjects were asked to walk barefoot at a self-selected speed over a 10-m walkway. Ground reaction forces were collected with two AMTI OR6-5 force plates (Advanced Medical Technology, Watertown, Massachusetts) and recorded at 1000 Hz.

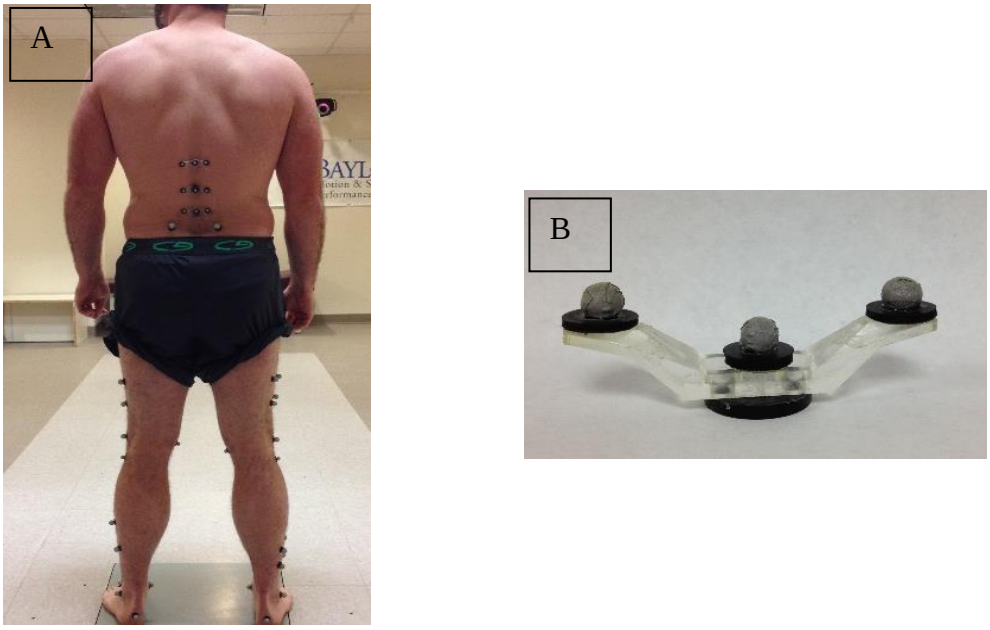

Figure 15 FV gait analysis preparation

A minimum of twenty gait cycles was used and averaged for statistical analysis.

The standing trial was used to create the model, and three-dimensional joint angles were determined using a Cardan x-y-z (flexion/ extension, abduction/adduction, longitudinal rotation) rotation sequence. The hip joint, segments L5, L3 and T12 motions were defined relative to the pelvis segment. The orientation of the pelvis segment was defined relative to the global (laboratory) coordinate system. The phases of the gait cycle, in percentage from 0 to 100% of the cycle were defined according to previously work by Perry.[68] As it follows: Heel strike (0); Loading response (0-20%); Mid-stance (20%-30%); Terminal stance (30%-50%); Preswing (50%-60%); Initial swing (60%-80%); Mid-swing (80%-90%); Terminal swing (90%-100%).

4B.2.5 Data Analysis

Student t-test was performed to compare the age, weight, height and BMI between the two groups. Fisher exact test was used to compare the gender between the two groups. Generalized linear mixed model (GLMM) was utilized to compare the gait measurements between the two groups adjusting to gait cycles (0, 1-10. 11-20, …., 91-100), the interaction between the groups and gait cycles and the effect of the individual (random effect). The data were analyzed using SAS/STAT® software version 9.4.

4B.3 Results

4B.3.1 Kinematic and Kinetic Differences Between DFVG and CG

Decreased femoral anteversion significantly ($p<0.05$) altered motion and alignment of the hip, pelvis, and spine segments (L5-L3-T12) during the entire gait cycle in at least one axis of

motion. (Table 7) DFAG also demonstrated a significantly ($P < 0.0001$) decreased ground reaction (GRF) force from heel strike to mid-stance and an increased GRF from mid-stance phase to pre-swing phase.

Table 7 Statistical Significances of Differences Between Groups

	P-Value (100% Gait cycle)	**P-Value (% Gait cycle)**	**Random Effect**
T12 Sagittal	0.1416	**<.0001** (0-60%)	**<.0001**
T12 Coronal	**0.0238**	**<.0001** (20-50%)	**<.0001**
T12 Transverse	0.536	**<.0001** (50-80%)	**<.0001**
L3 Sagittal	0.445	**<.0001** (10-80%)	**<.0001**
L3 Coronal	**0.0193**	**<.0001** (20-60%)	**<.0001**
L3 Transverse	0.1258	**<.0001** (10-40%)	**<.0001**
L5 Sagittal	0.6833	**<.0001** (10-40%)	**<.0001**
L5 Coronal	**<.0001**	**<.0001** (20-70%)	**<.0001**
L5 Transverse	**0.0128**	**<.0001** (0-60%)	**<.0001**
Pelvic Sagittal	**0.049**	**<.0001** (20-50%)	**<.0001**
Pelvic Coronal	0.6703	**<.0001** (20-60%)	**<.0001**
Pelvic Transverse	0.8819	**<.0001** (40-50%)	**<.0001**
Hip Sagittal	0.0968	**<.0001** (20-60%)	**<.0001**
Hip Coronal	0.6234	**<.0001** (70-80%)	**<.0001**
Hip Transverse	**0.002**	**<.0001** (30-60%)	**<.0001**
GRF	0.4894	**<.0001** (10-40%)	**<.0001**

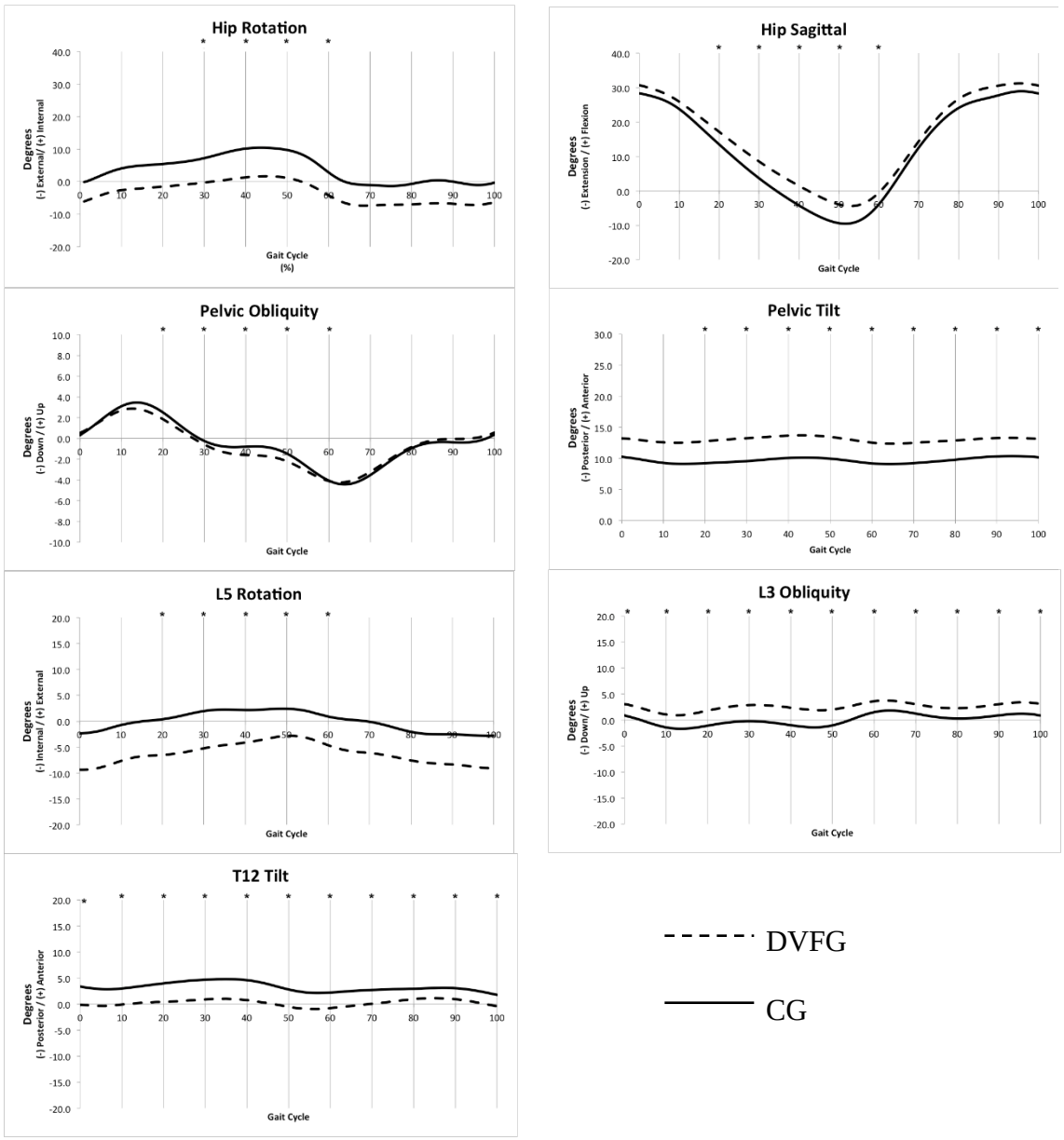

Figure 16 FV Gait analysis data

4B.3.2 Hip Joint

In the coronal plane, subjects with decreased femoral anteversion presented significantly ($p < 0.0001$) increased hip abduction from initial swing phase to mid swing phase. In the transverse

plane, the DFAG presented a significantly ($P = 0.002$) increased hip external rotation during the entire gait cycle, with significant differences ($P < 0.0001$) occurring from terminal stance to pre-swing phase. In the sagittal plane DFVG presented a significantly ($P < 0.0001$) decreased hip extension from mid-stance phase to pre-swing phase of gait.

4B.3.3 Pelvis

In the coronal plane, subjects with decreased femoral anteversion presented a significantly ($P < 0.0001$) increased ipsilateral pelvic drop from mid-stance to pre-swing phase. In the transverse plane, DFAG demonstrated a significantly ($P < 0.0001$) decreased contralateral pelvic rotation in the heel off phase. In the sagittal plane, DFVG demonstrated significantly ($P < 0.0001$) increased pelvic tilt during the entire gait cycle, with a greater difference between mid-stance to terminal stance.

4B.3.4 Spine (T12, L3, L5)

In the coronal plane, the DFAG presented significantly increased and constant ipsilateral inclination of T12 ($P = 0.0238$), L3 ($P = 0.0193$) and L5 ($P < 0.0001$) during the entire gait cycle. A significantly ($P < 0.0001$) increased contralateral rotation in the transverse plane were present by T12 from terminal stance to mid-swing, L3 from loading response to terminal stance and L5 from loading response to pre-swing. Segment L5 demonstrated a significantly ($P = 0.0128$) increased contralateral rotation and positioning during the entire gait cycle. In the sagittal plane, T12, L3 and L5 showed a significant ($P < 0.0001$) posterior tilt from loading response to pre-swing

Temporo-spatial data also revealed significant differences ($P < 0.05$) between the DFAG and CG for a slower walking speed (104.3 SD 25.88 *vs* 122.9 SD 12.42) and a shorter step length (right, 57.8 SD 11.34 *vs* 66.6 SD 3.99; left 57.6 SD 10.10 *vs* 66.45 SD 4.04).

4B.4 Discussion

The present study demonstrates decreased femoral anteversion affecting the hip, pelvis and spine (T12, L3, L5) biomechanics during gait, compared to a normal population. Decreased femoral anteversion demonstrated limited terminal hip extension during terminal stance to pre-swing phases of gait and an external foot progression angle during the entire gait cycle. The external foot progression angle compensation is well recognized; however, the loss of terminal hip extension is a new finding. DFVG demonstrated significantly increased anterior pelvic tilt during the entire gait cycle. Increased ipsilateral pelvic drop from mid-stance to pre-swing phase and a decreased contralateral pelvic rotation in the heel off phase were also observed. In the spine segments, an increased and constant ipsilateral inclination of T12, L3 and L5 during the entire gait cycle was statistically observed. The segment L5 demonstrated an increased contralateral rotation and positioning during the entire gait cycle. Additionally, the spine segments T12, L3 and L5 presented a posterior tilt from heel-strike to toe-off of the gait cycle. The hypothesis of the present study was confirmed with decreased femoral anteversion demonstrating significant differences in all three planar axes of the hip joint, pelvis and spine segments (T12, L3, L5) motion during gait. (Table 7)

The biomechanical relationship between the hip, pelvis, and spine has been clinically and biomechanically investigated under normal and pathological conditions.[7,39–45,69,70] Previous

investigations demonstrate an asymmetric hip ROM between internal/external rotation and excessive hip external rotation greater than internal rotation in subjects with low back pain symptoms and sacroiliac joint dysfunctions.[44,45,71,72] Femoral anteversion plays an important role influencing hip ROM discrepancies and may be a predicting factor for low back pain development. Clinical applications should consider the influence of hip ROM abnormalities on low back biomechanics. Patients with low back pain would benefit from a hip examination and an evaluation of the femoral anteversion.

The orientation of the femoral head/neck due to decreased femoral anteversion and its influences in proximal load transfer to the lumbopelvic segments are the key factors in understanding the effects of decreased femoral anteversion on gait. Despite the lack of significant differences between groups, DFAG presented a smaller GRF from heel-strike to mid-stance phases of gait. Previous biomechanical studies had observed the same phenomenon in the gait of children with cerebral palsy and adults with total hip replacements. As femoral anteversion increases, an increased hip contact force was produced and an increased moment in the coronal plane.[61,73,74] This factor can explain the significantly decreased terminal hip extension shown by the DFAG in this study. The magnitude of the force vector anterior to the hip joint center determines the necessary amount of hip extensor moment from heel strike to terminal stance for the initiation of hip extension during gait.[68]

The DFAG showed a prominent external rotation of the hip during the entire gait cycle in the present work, which is consistent with the literature. Studies have speculated increased external rotation may be to avoid premature contact between the femur and the acetabulum, increase hip joint reaction forces, and provide energy efficiency by the hip extensors and abductors muscles.[38,50,68,75,76] An excessive hip external rotation may also release the tension at

the iliofemoral ligament, which limits hip internal rotation during hip flexion angles (30°), and the iliofemoral ligament, which limits hip internal and external rotation during extension (10°).[38] Therefore, hip external rotation and increased anterior pelvic tilt may release the iliofemoral and ischiofemoral ligament tension.[38] Recently, Gómez-Hoyos et al. simulated a hip-spine model of the influence of altered femoral anteversion and iliofemoral ligament on lumbar facet joint load. A release of the medial arm of the iliofemoral ligament significantly decreased lumbar (L3-4 and L4-5) spine facet joints pressure during 20 degrees of hip extension with the hip in retroverted and native state of anteversion. This anatomical study provides an explanation for joint alignment and soft tissue influences under axial load.

The DFAG spine segments (T12, L3 and L5) demonstrated significant differences in triaxial motion during gait. All spine segments presented constant and increased ipsilateral inclination and a small but significant contralateral T12 and L3 rotation in specific gait cycles that involved loading. An increased L5 contralateral rotation during the entire gait cycle was also observed. The spine followed the pelvic drop pattern in the coronal plane, which compensates for the lack of pelvic rotation in the transverse plane. Both patterns were observed in previous gait studies that have shown a strong lumbopelvic relationship in the coronal and transverse planes as a summation between pelvis and spine rotation.[68,77] The spine functional motion as a coupled effect behavior during associated axial rotations-lateral bending was demonstrated by Panjabi et.al in cadaveric experiments based on a clinical observation of patients will low back pain.[78–81] The soft tissue integration and joint connection contributes to load transfer and will affect the motion and alignment in adjacent segments, thus producing joint compensation and alignment abnormalities as demonstrated by the present work.

The pelvis is the base for the spine stability and any changes in pelvic position and anatomy can cause spinal compensation. The static sagittal plane balance of the hip-pelvic alignment influences the curve of the lumbar spine. In static position an increased anterior pelvic tilt produces an increased lumbar lordosis, while an increased posterior tilt produces a flat lumbar curve.[41,82,83] The present study demonstrated the opposite effect of the static model. The T12, L3, and L5 spine segments demonstrated a posterior spine tilt with more significant differences during the load phase, suggesting a "swayback" posture during gait related to a permanent increased anterior pelvic tilt. This vertebral positioning produces an anterior projection of the center of force oriented directly through the vertebral bodies and disc. Consequently, decreasing spine facet joints load and increasing spine mobility. In the transverse and coronal plane this mechanism of spine hypermobility is frequently found in cases of early disc degeneration and lumbar intra-facet osteoarthritis.[79,82,84]

The present findings have a direct clinical implication for those subjects with decreased femoral anteversion. The altered lumbopelvic motion associated to decreased terminal hip extension and increased external rotation will affect the load transfer, joint alignment and muscular activation. Additionally, an epidemiologic study investigating the distribution of low-back pain symptoms among subjects with decreased femoral anteversion would contribute to the literature.

4B.5 Limitations

The present study has important limitations. Subjects in the DFAG were recruited from a specialized orthopedic clinic after a physical examination for hip pain. Although the subjects

were asked to perform the experiment only if their gait was asymptomatic for hip pain. The range of femoral version in the DFAG was -14° to 7°. The wide range of 21° may account for the differences in gait between subjects revealed by post-hoc analysis. A study defining a specific range of decreased femoral anteversion may be needed to determine patterns of gait for this altered hip morphology.

4B.6 Conclusion

These biomechanical effects of femoral anteversion on hip, pelvis and spine motion shows the importance of hip femoral anteversion screening on spine and pelvic disorders. The present study demonstrated decreased femoral anteversion as a morphologic hip abnormality influencing proximal adaptations from the hip joint to the pelvis and spine.

Chapter 5

Aim 4: Finite element analysis of ischiofemoral impingement, cam-type femoroacetabular impingement, and increased/decreased femoral version

5.1 Introduction

The hip pathologies simulated in benchtop cadaveric experiments in Aim 1, Aim 2, and Aim 3 were developed to evaluate with finite element analysis (FEA). Finite element techniques will further validate and confirm the lumbar spine effects resulting from the hip pathologies studied.

5.2 Materials & Methods

5.2.1 Osseous Geometry Segmentation

Osseous geometry was developed using CT imaging of a cadaveric specimen. 3D Slicer was used to segment osseous geometry of the femur, pelvis, sacrum, L5, L4, and L3 spine segments. Osseous segments were then modified using Blender to remove extraneous artifacts and perform smoothing. Additional smoothing and post-processing were performed in MeshMixer software to obtain final STL files. STL files were then reverse engineering in ANSYS v19 using the skin

Figure 17 FEA osseous geometry

surfacing tool to reduce number of surface elements. Final geometry was assembled in Creo v5. (Figure 17)

5.2.2 Soft Tissue Attachments

Soft tissue will be included in the FE model to simulate native musculoskeletal conditions. The following soft tissue structures will be included: Gluteus Maximus, Psoas Major, Adductor Longus, Rectus Femoris, Biceps Femoris. The soft tissue chosen are instrumental musculotendinous structures involved in normal gait. (Figure 18)

The soft tissue will be modeled as springs to reduce the computational time required to solve the finite element model. The materials properties are based on the Youngs modulus, cross-sectional area, and length of the muscle as determined by Ward et al.[85] (Table 8)

Table 8 FEA soft tissue spring material properties

	E (N/m^2)	**A(m^2)**	**L(m)**	**k = [(A*E)/L] (N/m)**
Gluteus Maximus	18510	3.30E-03	0.2695	226.6530612
Psoas Major	18510	7.70E-04	0.2425	58.77402062
Adductor Longus	18510	6.50E-04	0.2184	55.08928571
Rectus Femoris	18510	1.35E-03	0.3628	68.87679162
Biceps Femoris	18510	1.13E-03	0.3473	60.2254535

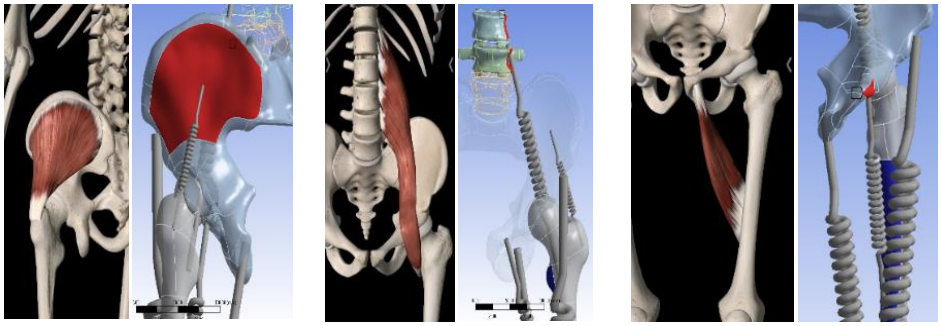

Figure 18 FEA soft tissue modeled as springs

5.2.3 Material Properties

Material properties for osseous geometry were modeled as orthotropic linear elastic materials. Intervertebral disk and muscle were modeled as isotropic linear elastic materials. (Table 9)

Table 9 FEA material properties assigned

	Density (kg m^-3)	Youngs Modulus ('E')	Poisson (v)	Ex	Ey	Ez	v(x)	v(y)	v(z)	Shear Modulus XY	Shear Modulus YZ	Shear Modulus XZ
Bone	1850			1.16 E+10	1.22 E+10	1.99 E+10	0.42	0.23	0.23	4.00 E+09	5.00 E+09	5.40 E+09
IVD	1100	8.00 E+06	0.45									
Muscle	1060	18510	0.499									

5.2.4 Meshing

Meshing was performed using quadratic elements assigned to all segments with maximum tetrahedral size of 15mm and minimum size of 5mm. Contact sizing of 3mm was assigned to all contact elements to further refine the mesh.

5.2.5 Data Collection

Finite element analysis was performed in conjunction with cadaveric benchtop methods. Resultant data collected was obtained from regions specific to sensor elements used in the cadaveric experiments. Ischiofemoral impingement and increased/decreased femoral version data was collected in the facet joint of the required L3, L4, or L5 lumbar spine segment. Specifically, nodes were selected on the facet joint within 1 cm to mimic the sensing location of the Tekscan force sensors used in cadaveric experiments. (Figure 19) A new geometric coordinate system was created at each facet joint so that the positive ‘x’ coordinate is normal to the surface.

Baseline data and corresponding ischiofemoral impingement and increased/decreased femoral version for ‘Sum of Forces in ‘X’’ direction and ‘Equivalent Stress’ was collected. The ‘Frictionless’ boundary condition was used for Ischiofemoral impingement and increased/decreased femoral version finite element analyses, in addition to the control data.

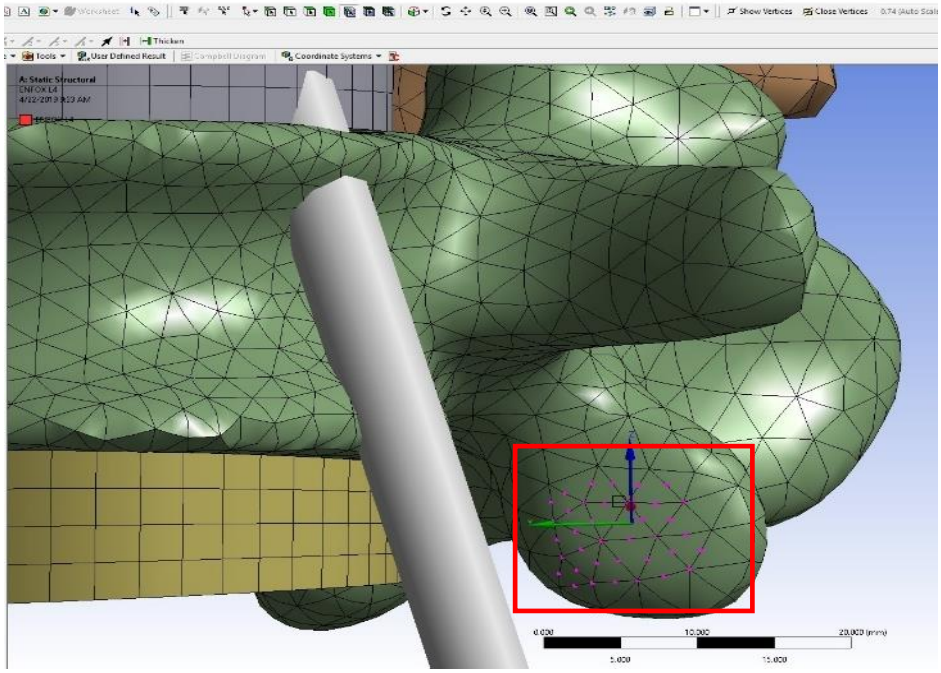

Figure 19 FEA data collection technique

Collected data for Femoroacetabular impingement was obtained for whole L3, L4, and L5 IVD segments. ‘Sum of Forces’ and ‘Total Deformation’ data was collected for the IVD segments. The FAI, and associated control, collected data was from the ‘Joint’ boundary condition.

5.3 Results

5.3.1 Ischiofemoral impingement FEA results

Baseline data for ischiofemoral impingement is considered as no impingement between the ischium and lesser trochanter. Sum of forces in the facet joints for L3-L4, L4-L5, L5-S1 was measured to be 0.38, 8.60, and 4.44 N, respectively, for 10 degrees hip extension. Sum of forces in the facet joint for L3-L4, L4-L5, and L5-S1 was measured to be 0.60, 7.69, and 5.08 N, respectively during 20 degrees of hip extension. Equivalent stress was measured to be 0.27, 2.82, 1.69 MPa for 10 degrees hip extension and 0.76, 7.19, and 3.88 MPa for 20 degrees hip extension. (Figure 20)

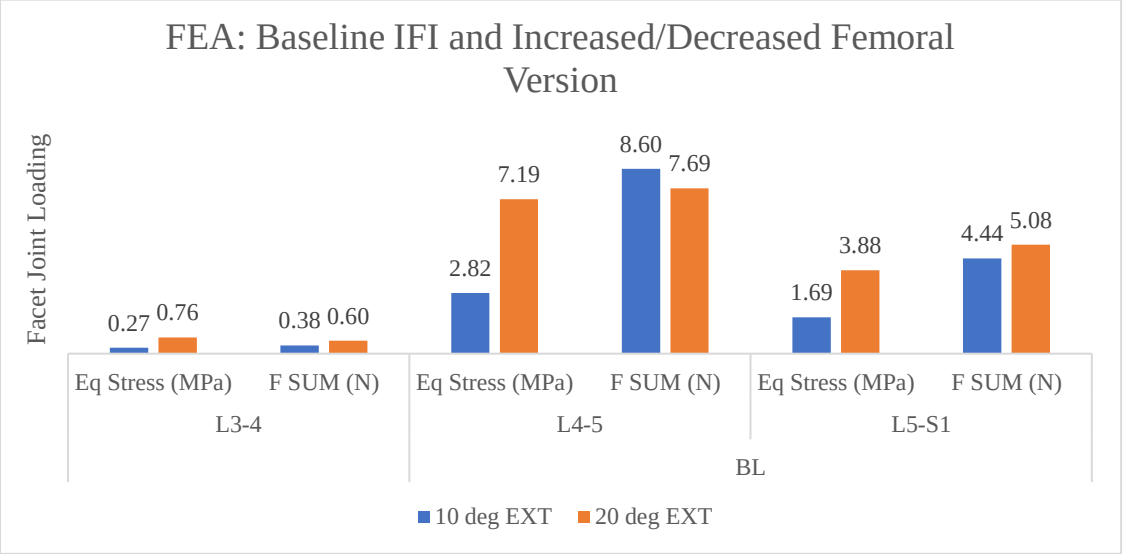

Figure 20 FEA baseline IFI and FV facet joint loading

Ischiofemoral impingement increased loading in all spine segment facet joints. Sum of forces was determined to be 0.79 N, 10.54 N, and 8.61 N for the L3-4, L4-5, and L5-S1 facet joints for 10 degrees hip extension. Hip extension to 20 degrees further increased the lumbar

facet joint loading. Similar to the baseline data, maximum loading (21.91 N) was observed during 20 degrees hip extension in the L4-L5 facet joint. (Figure 21)

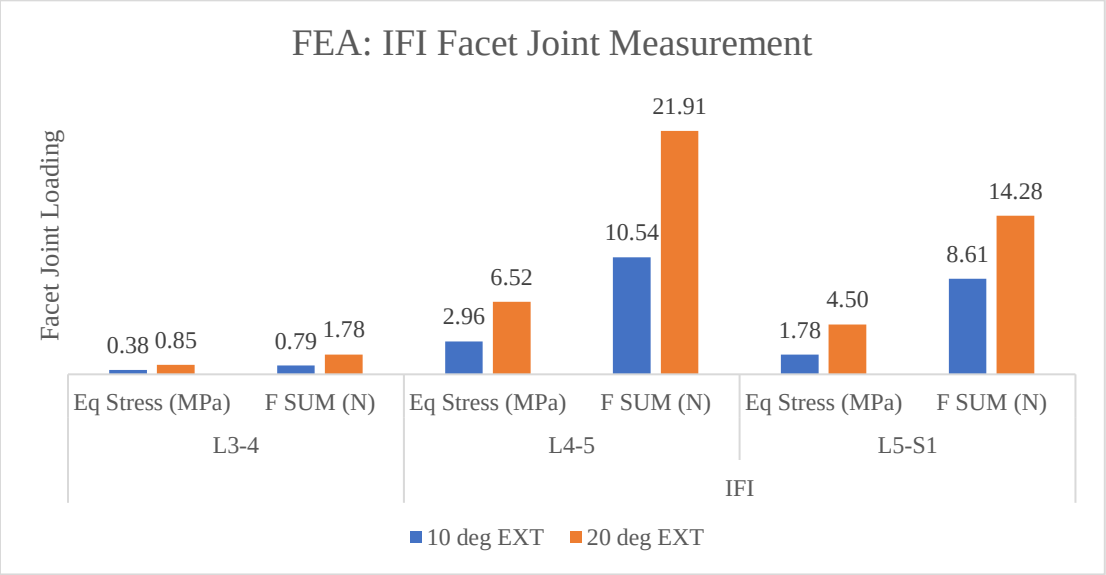

Figure 21 FEA IFI facet joint measurement

5.3.2 Femoroacetabular impingement FEA results

Baseline IVD data was obtained from L3, L4, and L5 IVD segments. Sum of forces was measured for direct comparison to cadaveric data. An incremental increase in sum of forces was observed during 90- and 90+IR-degrees hip flexion in the L3 (0.50 N; 0.50N) and L4 (0.84 N; 0.86N) IVD. The largest sum of forces was observed in the L5 IVD for both 90 degrees (6.49N) and 90+IR degrees (5.75N). (Figure 22) Hip flexion to 120 degrees and 120+IR continued to increase IVD loading, with the largest loading observed in the L5 IVD (16.69N; 17.06N). The observed sum of forces in the L3 IVD was 0.0003 N and 0.00025 N for 120 degrees and 120+IR degrees hip flexion, respectively. Further quantification of FEM methods is represented by total deformation results. The L5 IVD segment resulted in the largest loading, as seen in cadaveric specimens. (Figure 23)

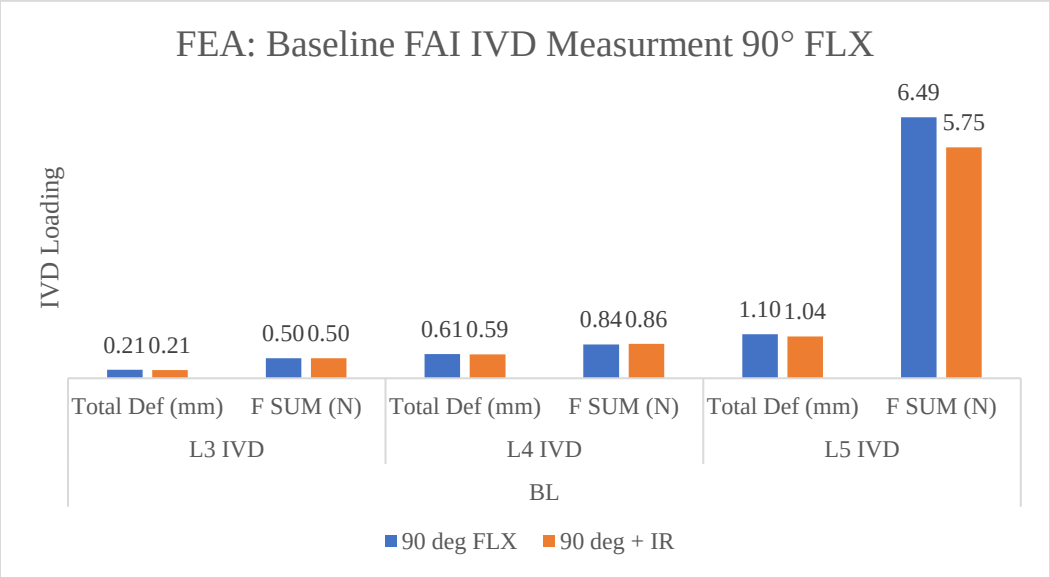

Figure 22 FEA baseline FAI IVD loading 90 FLX

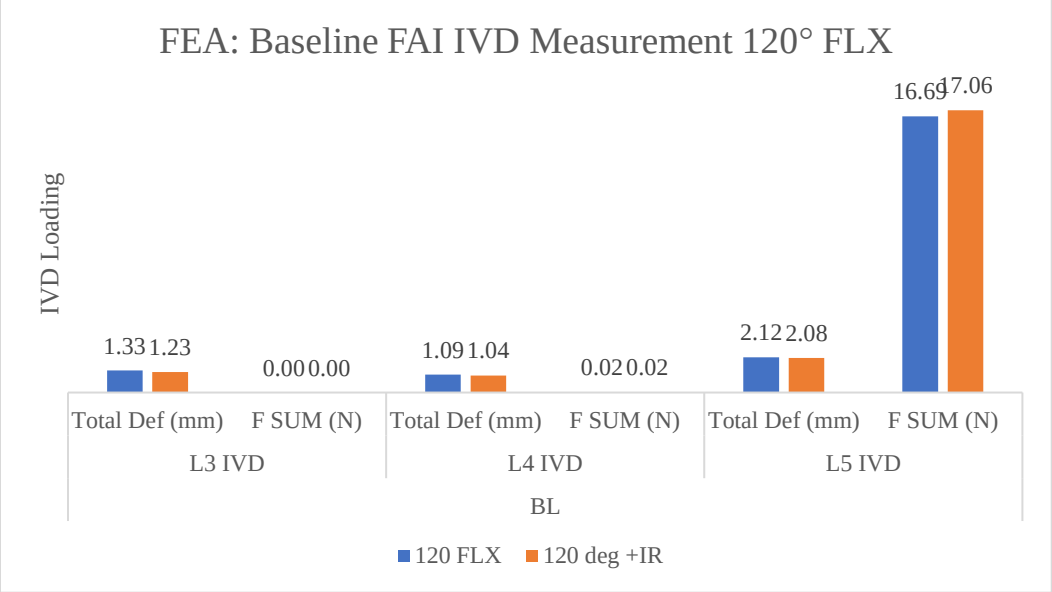

Figure 23 FEA baseline FAI IVD loading 120 FLX

Simulated FAI increased the loading in all lumbar spine segments. During 90 degrees hip flexion the sum of forces increased from 0.1 N at the L3 IVD to 5.05 N at the L4 IVD to 21.02 N at the L5 IVD. 90+IR degrees hip flexion increased IVD loading in the L3 and L5 IVD

segments, however a slight decrease was observed in the L4 IVD. This deviation is mostly attributed to excessive motion observed in this region and the lack of interspinous supports. (Figure 24) Loading in all three lumbar IVD segments increased during hip flexion to 120 degrees. The decrease observed for 120+IR hip flexion is attributed to the added pinball region which was required to obtain solution convergence. Without the pinball region, the excessive motion and displacement in the lumbar IVD segments prevented solution convergence. This data supports cadaveric experiment findings. As seen in the baseline measurements, the L5 IVD segment resulted in the largest loading. (Figure 25)

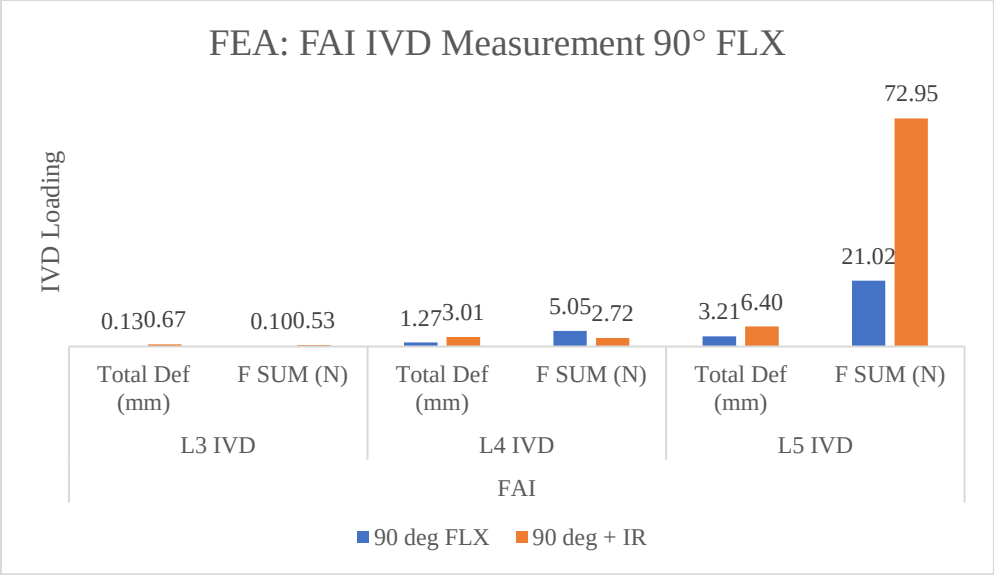

Figure 24 FEA FAI IVD loading 90 FLX

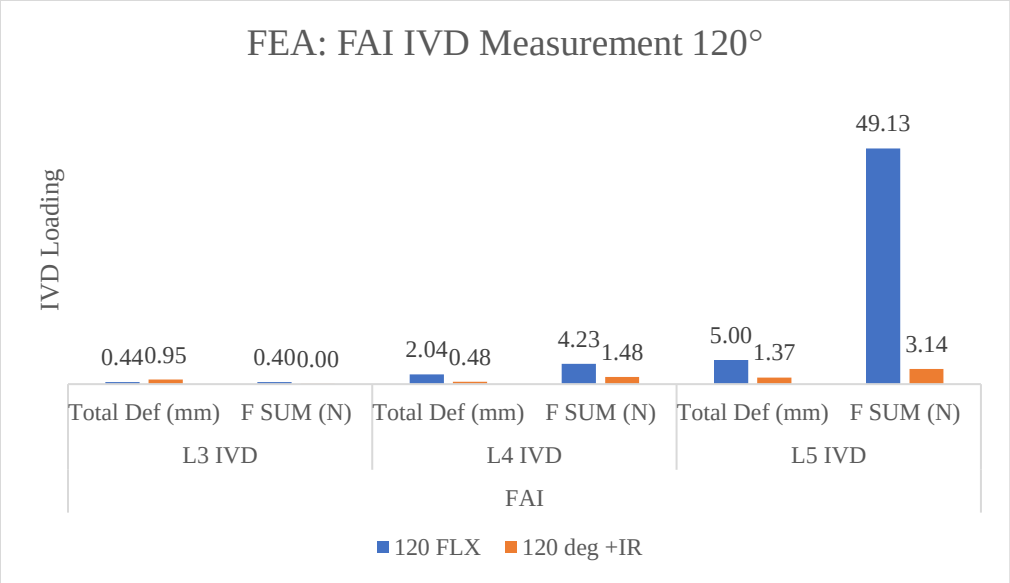

Figure 25 FEA FAI IVD loading 120 FLX

5.3.3 Increased/decreased femoral version FEA results

Decreased femoral version (-10 degrees) reflected similar decrease in facet joint loading as seen in cadaveric experiments. (Figure 26)

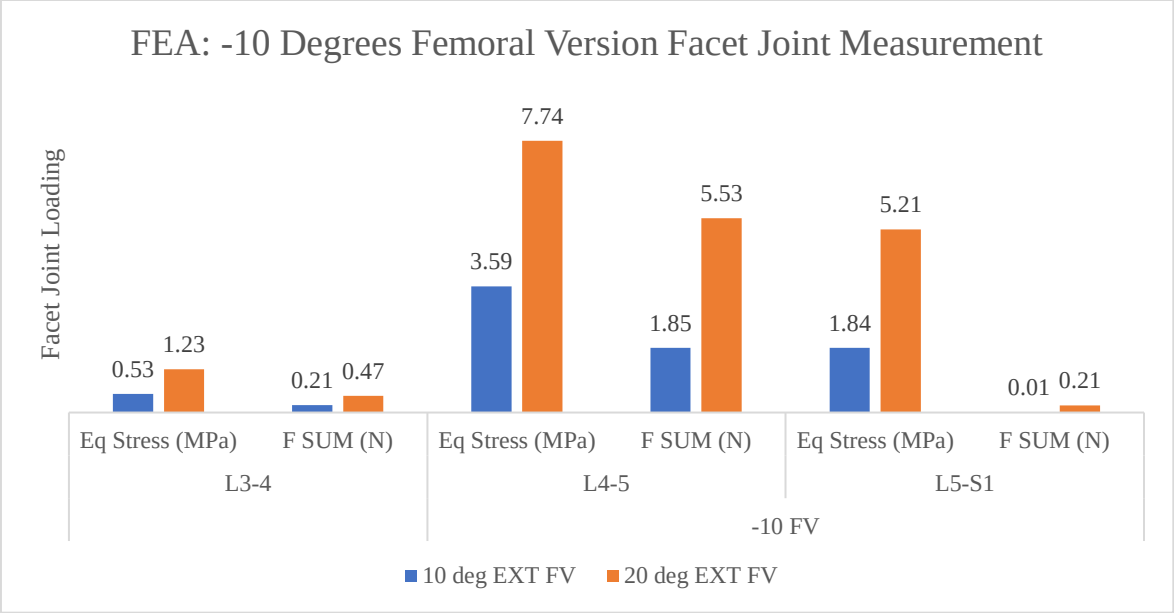

Figure 26 FEA FV -10 degrees facet joint loading

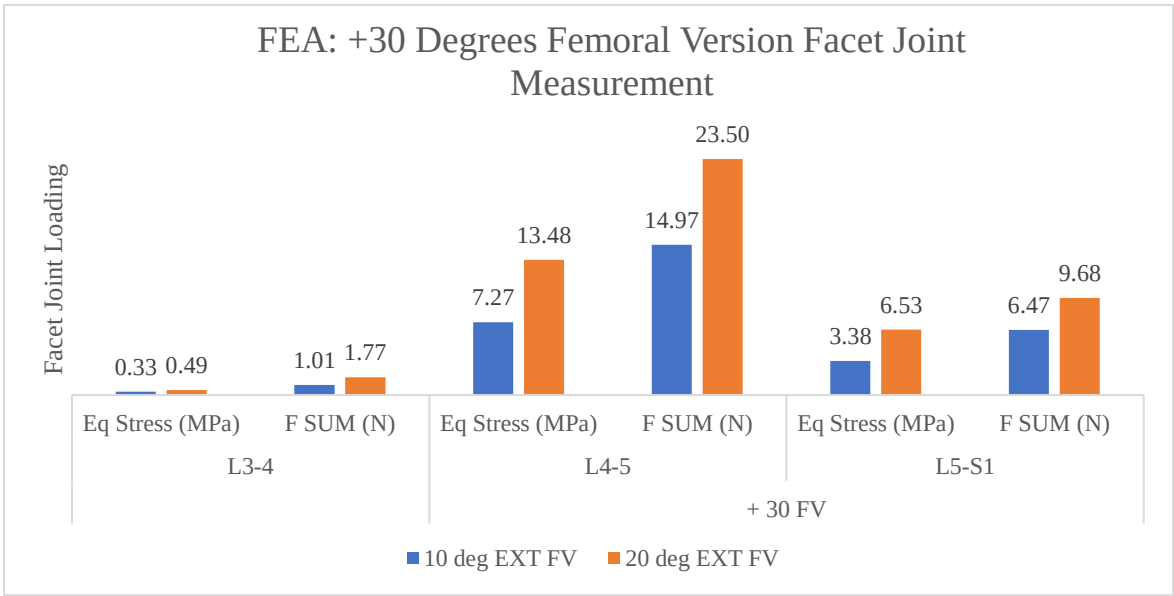

Figure 27 FEA FV +30 degrees facet joint loading

The resultant data for +30 degrees simulated femoral version increased facet joint loading, when compared the native state. This data reflects a similar increase in facet joint loading experienced during cadaveric testing. (Figure 27)

5.4 Discussion

Finite element analysis of ischiofemoral impingement, femoroacetabular impingement, and increase/decreased femoral version provided significant additional data to support the cadaveric findings. Similar trends with increasing or decreasing loading was observed in comparison to cadaveric trends. A strength of the finite element model is the incorporation of native osseous geometry and material properties. Soft tissue attachments were necessary to re-create the complex kinematic chain relationship between the hip joint and lumbar spine. Not only does the data support cadaveric experiments, the finite element analysis model developed provides a strong foundation for future research utilizing these techniques.

Finite element analysis serves as an ideal tool for biomechanics investigations, however the technique has not been extensively utilized in the field of hip preservation. In regard to the hip joint, finite element analysis is predominantly utilized for studying total hip replacement mechanics. The rapid attention in hip preservation and biomechanics has stimulated researchers to integrate finite element techniques for the study of hip impingement pathologies. Ng et al. utilized finite element techniques to investigate the maximum shear stress and location of cam-type FAI during squatting.[86] The authors conclude peak maximum shear stress occurs on the underlying bone as opposed to directly affecting the cartilage. An early finite element analysis of impingement and dysplasia was produced by Chegini et al.[87] The authors concluded stresses

within the soft tissues of the hip joint are influenced by bony anatomy in addition to activity type. The presented finite element analysis of IFI, FAI, and FV not only validates the cadaveric benchtop experiments, but expands on published findings that report a negative effect of hip impingement.

Data collection methods for the finite element analysis underwent several iterations. The model was developed to simulate cadaveric benchtop experiments, however a reduction in musculotendinous and neurovascular structures was necessary to achieve solution convergence. Eliminating these structures allowed for more efficient solutions and developed promising results to support the benchtop experiments. However, the reduction of the many important soft tissue connections can explain for the marked difference in overall values when comparing the cadaveric results to the finite element results.

The data collection technique for FAI simulations differed from the IFI and increased/decreased FV simulations. Data for the IFI and FV simulations were collected at nodes on the facet joints with a 10 mm diameter to reflect the sensing element. A new coordinate system was created at each facet joint so that the ‘x’ direction was normal to the surface of the facet joint. This allowed to collect the sum of forces in the ‘x’ direction. The method simulates the piezoresistive force sensor that was used for cadaveric experiments. However, this method was not effective for FAI measurements on the IVD. The facet joints are a smaller, localized face, and affected by the facet of the adjacent vertebral segment. In comparison, the IVD are much larger and therefore the maximal loading can occur at multiple faces of the disk. Early techniques for extracting FAI IVD data incorporating a midplane cross-section through the IVD. This was performed to mimic how the sensing elements were inserted directly into the IVD. (Figure 28) A Force reaction probe was then inserted to measure the force in this region. Due to

the large deformation associated with deep hip flexion and internal rotation, the resultant data not accurately represent the mechanics occurring in this region. Additionally, when comparing the force reaction results, and sum of forces on the superior or inferior IVD faces, there was a large discrepancy in the results.

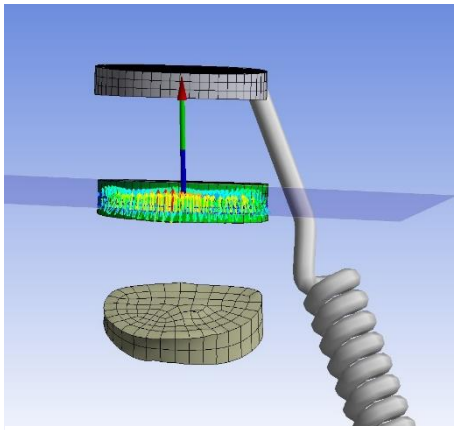

Figure 28 FEA midplane measurement technique

The decision to use the sum of forces in the entire IVD allows for a global representation of the mechanics. Several of the key soft tissue structures not included in the model are the interspinous ligaments. These ligaments are strong thick attachments to the vertebral segments to protect excessive movement.

The largest motion and primary generator of abnormal biomechanics is due to abnormal sagittal plane motion during hip flexion, especially in the FAI simulations. Obtaining converged results for FLX 120 +IR proved to be a difficult task for the model. Elimination of the necessary soft tissue attachments created excessive motion within the lumbosacral complex resulting in non-convergence. To remedy the issue for this one case, a pinball region of 15 mm was incorporated into the connections at the L4-L5 connection, and L5-S1 connection. (Figure 29)

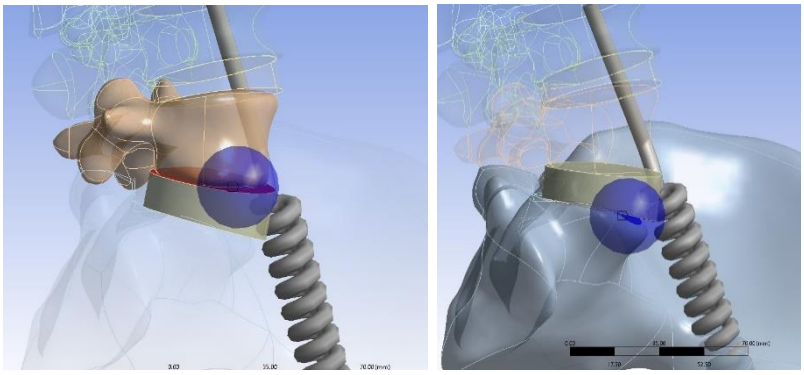

Figure 29 FEA pinball addition for 120+IR FLX

5.5 Conclusion

Finite element analysis models were successfully developed to simulate ischiofemoral impingement, femoroacetabular impingement, and increased/decreased femoral version to validate cadaveric experimental conditions. Data obtained from the FEA models of abnormal hip pathology accurately support the cadaveric benchtop experiments presented in aims 1, 2, and 3.

Chapter 6

Conclusions and Future Directions

6.1 Conclusions

Understanding of the hip joint has undergone a significant transformation in recent years due to the increased interest in hip preservation techniques. Abnormal pathologies including ischiofemoral impingement, femoroacetabular impingement, and abnormal femoral version are now commonly diagnosed, however the underlying biomechanics of the abnormal hip pathologies are poorly understood. The aim of the presented work was to investigate the biomechanics of the abnormal hip pathologies and the effects on the lumbar spine. To accomplish this goal several experimental and analytical techniques were utilized including cadaveric benchtop experiments, motion and gait analysis, retrospective clinical data, and finite element analysis.

The cadaveric benchtop experiments served to provide a foundation for simulating the abnormal hip pathologies and observing effects in the lumbar spine. The presence of ischiofemoral impingement increased loading in the lumbar spine facet joints when compared to a native condition during hip extension to 10 and 20 degrees. An increase in lumbar intervertebral disk loading was observed in the presence of cam-type femoroacetabular impingement during hip flexion and internal rotation movements to 90 and 120 degrees. A decrease in facet joint loading was observed in the presence of decreased femoral version (-10 degrees), however increased femoral version (+30 degrees) increased overall lumbar facet joint loading during hip extension to 10 and 20 degrees, when compared to a native state. The biomechanical effects of decreased femoral version were further explored using motion capture

and gait analysis techniques. Significant changes in lumbopelvic motion were observed in patients with clinically diagnosed decreased femoral version when compared to normal femoral version patients.

The integration of finite element analysis techniques was a significant strength to the overall goal of establishing a hip-spine connection between abnormal hip pathology and the lumbar spine. To date finite element analysis has focused on the femoro-pelvic region. This was the first study to incorporate the kinematic chain to lumbo-pelvic biomechanics. The data obtained from the finite element analyses validated the findings of cadaveric benchtop experiments for all cases of hip pathologies studied. The presented data serves as a strong foundation to continue using computational methods to describe the intricate biomechanics of the lumbopelvic complex.

6.2 Future Directions

The experimental methods and results presented in this dissertation give rise to several directions for future work. Integration of motion capture technology for cadaveric benchtop experiments will allow for more quantitative data regarding lumbo-pelvic motion during hip flexion and extension. This data is necessary to develop a comprehensive understanding of the lumbo-pelvic kinematics in the presence of abnormal hip pathologies, in conjunction with force sensing data presented. Advancements in robotic technology can be implemented for manipulation of hip flexion and extension movements for cadaveric research. This will help to normalize motion cycle timing, in addition to obtaining valuable torque and force resistance measurements.

The finite element analysis techniques presented are a strong foundation for future directions. The limited soft tissue connections incorporated in the models provided the kinematic chain reaction, however additional soft tissue should be included in future studies. Transient dynamic analysis can also be incorporated to understand the effects in the lumbar spine over time as opposed to the static structural model developed. Additionally, finite element analysis can be utilized to investigate the effects of ligamentous, muscular, and neural structures in the kinematic chain during hip flexion and extension.

Significant work remains to accurately understand the role of the hip joint on back pain. The presented work focused primarily on lumbar pain, however the methods can be applied to study the effects in the thoracic and cervical spine segments. Additional future work can be directed at the effects of abnormal hip anatomy on structures below the hip, including the knee joint. Pilot gait analysis experiments performed by the Hip Preservation Center suggest a similar deleterious effect of abnormal hip pathology on the knee joint.

REFERENCES

1. Huijbregts P. Lumbopelvic region: Anatomy and biomechanics. *Wadsworth C HSC 112 Curr Concepts Orthop Phys Ther*. 2001.
2. Filler AG. Piriformis and Related Entrapment Syndromes: Diagnosis & Management. *Neurosurg Clin N Am*. 2008;19(4):609-622. doi:10.1016/j.nec.2008.07.029
3. Offierski CM, Macnab MB. Hip-Spine Syndrome. *Spine (Phila Pa 1976)*. 1983;8(3):316-321.
4. Ben-Galim P, Ben-galim T, Rand N, et al. Hip-Spine Syndrome The Effect of Total Hip Replacement Surgery on Low Back Pain in Severe Osteoarthritis of the Hip. *Spine (Phila Pa 1976)*. 2007;32(19):2099-2102. doi:10.1016/j.humov.2006.08.002
5. Fogel GR, Esses SI. Hip spine syndrome : management of coexisting radiculopathy and arthritis of the lower extremity. *Spine J*. 2003;3:238-241.
6. Matsuyama Y, Hasegawa Y, Yoshihara H, et al. Hip-spine syndrome: total sagittal alignment of the spine and clinical symptoms in patients with bilateral congenital hip dislocation. *Spine (Phila Pa 1976)*. 2004;29(21):2432-2437. http://journals.lww.com/spinejournal/Abstract/2004/11010/Hip_Spine_Syndrome__Total_Sagittal_Alignment_of.16.aspx. Accessed October 8, 2014.
7. Redmond JM, Gupta A, Hammarstedt JE, Stake CE, Domb BG. The hip-spine syndrome: How does back pain impact the indications and outcomes of hip arthroscopy? *Arthrosc - J Arthrosc Relat Surg*. 2014;30(7):872-881. doi:10.1016/j.arthro.2014.02.033
8. Lejkowski PM, Poulsen E. Elimination of intermittent chronic low back pain in a recreational golfer following improvement of hip range of motion impairments. *J Bodyw Mov Ther*. 2013;17(4):448-452. doi:10.1016/j.jbmt.2013.01.004
9. Schröder RG, Reddy M, Hatem MA, et al. A MRI study of the lesser trochanteric version and its relationship to proximal femoral osseous anatomy. *J Hip Preserv Surg*. 2015;2(4):410-416. doi:10.1093/jhps/hnv067
10. Ganz R, Parvizi J, Beck M, Leunig M, Notzli H, Siebenrock KA. Femoroacetabular Impingement: A Cause for Osteoarthritis of the Hip. *Clin Orthop Relat Res*. 2003;417:112-120. doi:10.1097/01.blo.0000096804.78689.c2

11. Birmingham PM, Kelly BT, Jacobs R, McGrady L, Wang M. The effect of dynamic femoroacetabular impingement on pubic symphysis motion: a cadaveric study. *Am J Sports Med*. 2012;40(5):1113-1118. doi:10.1177/0363546512437723
12. MIXTER WJ, BARR JS. Rupture of the Intervertebral Disc with Involvement of the Spinal Canal. *N Engl J Med*. 1934;211(5):210-215. doi:10.1056/NEJM193408022110506
13. Filler AG, Haynes J, Jordan SE, et al. Sciatica of Nondisc Origin and Piriformis Syndrome: Diagnosis by Magnetic Resonance Neurography and Interventional Magnetic Resonance Imaging with Outcome Study of Resulting Treatment. *J Neurosurg Spine*. 2005;2(2):99-115. doi:10.3171/spi.2005.2.2.0099
14. Filler AG. Diagnosis and treatment of pudendal nerve entrapment syndrome subtypes: imaging, injections, and minimal access surgery. *Neurosurg Focus*. 2009;26(2):E9. doi:10.3171/FOC.2009.26.2.E9
15. Martin HD, Shears S a, Johnson JC, Smathers AM, Palmer IJ. The endoscopic treatment of sciatic nerve entrapment/deep gluteal syndrome. *Arthrosc J Arthrosc Relat Surg*. 2011;27(2):172-181. doi:10.1016/j.arthro.2010.07.008
16. Hatem MA, Palmer IJ, Martin HD. Diagnosis and 2-Year Outcomes of Endoscopic Treatment for Ischiofemoral Impingement. *Arthrosc J Arthrosc Relat Surg*. 2015;31(2):239-246. doi:10.1016/j.arthro.2014.07.031
17. Gómez-Hoyos J, Schröder R, Reddy M, et al. Is There a Relationship Between Psoas Impingement and Increased Trochanteric Retroversion? *J Hip Preserv Surg*. 2015;2(2):164-169. doi:10.1093/jhps/hnv024
18. Vialle R, Levassor N, Rillardon L, Templier A, Skalli W, Guigui P. Radiographic analysis of the sagittal alignment and balance of the spine in asymptomatic subjects. *J Bone Jt Surg*. 2005;87-A(2):260-267. doi:10.2106/JBJS.D.02043
19. Perry J, Burnfield JM, Cabico LM. *Gait Analysis : Normal and Pathological Function*. SLACK; 2010.
20. Devin CJ, Mccullough KA, Morris BJ, Yates AJ, Kang JD. Hip-spine Syndrome. *J Am Acad Orthop Surg*. 2012;20:434-442.
21. Torriani M, Souto SCL, Thomas BJ, Ouellette H, Bredella M a. Ischiofemoral impingement syndrome: an entity with hip pain and abnormalities of the quadratus

femoris muscle. *AJR Am J Roentgenol*. 2009;193(1):186-190. doi:10.2214/AJR.08.2090

22. Popovich JM, Welcher JB, Hedman TP, et al. Lumbar facet joint and intervertebral disc loading during simulated pelvic obliquity. *Spine J*. 2013;13(11):1581-1589. doi:10.1016/j.spinee.2013.04.011
23. Roussouly P, Nnadi C. Sagittal plane deformity: an overview of interpretation and management. *Eur Spine J*. 2010;19(11):1824-1836. doi:10.1007/s00586-010-1476-9
24. Lamontagne M, Kennedy MJ, Beaulé PE. The Effect of cam FAI on Hip and Pelvic motion during maximum squat. *Clin Orthop Relat Res*. 2009;467(3):645-650. doi:10.1007/s11999-008-0620-x
25. Gómez-Hoyos J, Khoury AN, Schröder R, Johnson E, Palmer IJIJ, Martin HDHD. The Hip-Spine Effect: A Biomechanical Study of Ischiofemoral Impingement Effect on Lumbar Facet Joints. *Arthrosc - J Arthrosc Relat Surg*. 2016;33(1):101-107. doi:10.1016/j.arthro.2016.06.029
26. Tonnis D, Heinecke A. Acetabular and Femoral Anteversion : Relationship with Osteoarthritis of the Hip. *J Bone Jt Surg*. 1999;81(12):1747-1770.
27. Bedi A, Dolan M, Leunig M, Kelly BT. Static and Dynamic Mechanical Causes of Hip Pain. *Arthrosc J Arthrosc Relat Surg*. 2011;27(2):235-251. doi:10.1016/j.arthro.2010.07.022
28. Ng KCG, El Daou H, Bankes MJK, Rodriguez Y Baena F, Jeffers JRT. Hip Joint Torsional Loading Before and After Cam Femoroacetabular Impingement Surgery. *Am J Sports Med*. 2019;47(2):420-430. doi:10.1177/0363546518815159
29. Diamond LE, Wrigley T V., Bennell KL, Hinman RS, O'Donnell J, Hodges PW. Hip joint biomechanics during gait in people with and without symptomatic femoroacetabular impingement. *Gait Posture*. 2016;43:198-203. doi:10.1016/j.gaitpost.2015.09.023
30. Diamond LE, Bennell KL, Wrigley T V., Hinman RS, O'Donnell J, Hodges PW. Squatting biomechanics in individuals with symptomatic femoroacetabular impingement. *Med Sci Sports Exerc*. 2017;49(8):1520-1529. doi:10.1249/MSS.0000000000001282
31. Bagwell JJ, Snibbe J, Gerhardt M, Powers CM. Hip kinematics and kinetics in persons with and without cam femoroacetabular impingement during a deep squat task. *Clin Biomech*. 2015;31:87-92. doi:10.1016/j.clinbiomech.2015.09.016

32. Kennedy MJ, Lamontagne M, Beaulé PE. Femoroacetabular impingement alters hip and pelvic biomechanics during gait Walking biomechanics of FAI. *Gait Posture*. 2009;30:41-44. doi:10.1016/j.gaitpost.2009.02.008
33. Fader RR, Tao MA, Gaudiani MA, et al. The Roles of Lumbar Lordosis and Pelvic Sagittal Balance in Femoroacetabular Impingement. *Bone Joint J*. 2018;100(B):1275-1279. https://online.boneandjoint.org.uk/doi/pdf/10.1302/0301-620X.100B10.BJJ-2018-0060.R1?casa_token=u8O5ZQgT5T8AAAAA:YBx2WShhG8X690Z142Xl8UJOAsfjLyEOsUlBFEf_7lurSAY6hPo3G01DzUS02dtoAYK76pZb-qhm.
34. Jaumard N V, Welch WC, Winkelstein BA. Spinal facet joint biomechanics and mechanotransduction in normal, injury and degenerative conditions. *J Biomech Eng*. 2011;133(7):071010. doi:10.1115/1.4004493
35. Krebs DE, Robbins CE, Lavine L, Mann RW. Hip biomechanics during gait. *J Orthop Sports Phys Ther*. 1998;28(1):51-59. doi:10.2519/jospt.1998.28.1.51
36. Levangie PK, Norkin CC. *Joint Structure and Function: A Comprehensive Analysis*. 5th ed. Philadelphia: F.A. Davis Company; 2011.
37. Husson J-L, Mallet J-F, Huten D, Odri G-A, Morin C, Parent H-F. The lumbar-pelvic-femoral complex: applications in hip pathology. *Orthop Traumatol Surg Res*. 2010;96(4):S10-S16. doi:10.1016/j.otsr.2010.03.007
38. Martin HD, Savage A, Braly BA, Palmer IJ, Beall DP, Kelly B. The Function of the Hip Capsular Ligaments : A quantitative report. *Arthroscopy*. 2008;24(2):188-195. doi:10.1016/j.arthro.2007.08.024
39. Yoshimoto H, Sato S, Masuda T, et al. Spinopelvic alignment in patients with osteoarthrosis of the hip: a radiographic comparison to patients with low back pain. *Spine (Phila Pa 1976)*. 2005;30(14):1650-1657.
40. Ben-galim P, Ben-galim T, Rand N, Haim A. Hip-Spine Syndrome: The Effect of Total Hip Replacement Surgery on Low Back Pain in Severe Osteoarthritis of the Hip. *Spine J*. 2007;32(19):2099-2102.
41. Lazennec J-Y, Brusson A, Rousseau M-A. Hip-spine relations and sagittal balance clinical consequences. *Eur Spine J*. 2011;20 Suppl 5:686-698. doi:10.1007/s00586-011-1937-9
42. Matsuyama Y, Hasegawa Y, Yoshihara H. Hip-Spine Syndrome Total Sagittal Alignment

of the Spine and Clinical Symptoms in Patients With Bilateral Congenital Hip Dislocation. *Spine J*. 2004;29(21):2432-2437.

43. Gómez-Hoyos J, Khoury A, Schroder R, Johnson E, Palmer I MH. The hip spine effect: A biomechanical study of ischiofemoral impingement effect on lumbar facet joints. *J Arthrosc Relat Surg*. 2016;In Press.
44. Van Dillen LR, Bloom NJ, Gombatto SP, Susco TM. Hip rotation range of motion in people with and without low back pain who participate in rotation-related sports. *Phys Ther Sport*. 2008;9(2):72-81. doi:10.1016/j.ptsp.2008.01.002
45. Vad VB. Low Back Pain in Professional Golfers: The Role of Associated Hip and Low Back Range-of-Motion Deficits. *Am J Sports Med*. 2004;32(2):494-497. doi:10.1177/0363546503261729
46. Gulan G, Matovinović D, Nemec B, Rubinić D, Ravlić-Gulan J. Femoral neck anteversion: values, development, measurement, common problems. *Coll Antropol*. 2000;24(2):521-527.
47. Reikeras O. Femoral neck angles. *Acta Orthop Scand*. 1982;53(1954):775-779.
48. Murphy SB, Simon SR, Kijewski PK, et al. Femoral Anteversion. *J Bone Jt SurgeryBone Jt Surg*. 1987;69(8):1169-1175.
49. Crane L. MP. Femoral Torsion Its Relation to toeing-i and toeing-out. *J Bone Jt Surg*. 1959;41(3):421-428.
50. Satpathy J, Kannan a., Owen JR, Wayne JS, Hull JR, Jiranek W a. Hip contact stress and femoral neck retroversion: a biomechanical study to evaluate implication of femoroacetabular impingement. *J Hip Preserv Surg*. 2015;0(0):1-8. doi:10.1093/jhps/hnv040
51. Dolan MM, Heyworth BE, Bedi A, Duke G, Kelly BT. CT reveals a high incidence of osseous abnormalities in hips with labral tears. *Clin Orthop Relat Res*. 2011;469(3):831-838. doi:10.1007/s11999-010-1539-6
52. Allen D, Beaulé PE, Ramadan O, Doucette S. Prevalence of associated deformities and hip pain in patients with cam-type femoroacetabular impingement. *J Bone Joint Surg Br*. 2009;91(5):589-594. doi:10.1302/0301-620X.91B5.22028
53. BY D. Tonnis AH, Tönnis D, Heinecke A, BY D. Tonnis AH. Acetabular and Femoral

Anteversion : Relationship with Osteoarthritis of the Hip *. *J Bone Jt Surg*. 1999;81(12):1747-1770. doi:10.2106/JBJS.L.00710

54. Chuter VH, Janse De Jonge XAK. Proximal and distal contributions to lower extremity injury: A review of the literature. *Gait Posture*. 2012;36:7-15. doi:10.1016/j.gaitpost.2012.02.001
55. Schache AG, Bennell KL, Blanch PD, Wrigley T V. The coordinated movement of the lumbo-pelvic-hip complex during running: A literature review. *Gait Posture*. 1999;10(1):30-47. doi:10.1016/S0966-6362(99)00025-9
56. Shimada T. Factors affecting appearance patterns of hip-flexion contractures and their effects on postural and gait abnormalities. *Kobe J Med Sci*. 1996;42(4):271-290.
57. Whittle MW, Levinec D. Measurement of lumbar lordosis as a component of clinical gait analysis. *Gait Posture*. 1997;5:101-107.
58. Lewis CL, Sahrmann S a. Effect of posture on hip angles and moments during gait. *Man Ther*. 2015;Feb 20(1):176-182. doi:10.1016/j.math.2014.08.007
59. Bergmann G, Graichen F, Rohlmann a. Hip joint loading during walking and running, measured in two patients. *J Biomech*. 1993;26(8):969-990. doi:10.1016/0021-9290(93)90058-M
60. Bosmans L, Jansen K, Wesseling M, Molenaers G, Scheys L, Jonkers I. The role of altered proximal femoral geometry in impaired pelvis stability and hip control during CP gait: A simulation study. *Gait Posture*. 2016;44:61-67. doi:10.1016/j.gaitpost.2015.11.010
61. Bosmans L, Wesseling M, Desloovere K, Molenaers G, Scheys L, Jonkers I. Hip contact force in presence of aberrant bone geometry during normal and pathological gait. *J Orthop Res*. 2014;32(11):1406-1415. doi:10.1002/jor.22698
62. Radler C, Kranzl A, Manner HM, Höglinger M, Ganger R, Grill F. Torsional profile versus gait analysis: Consistency between the anatomic torsion and the resulting gait pattern in patients with rotational malalignment of the lower extremity. *Gait Posture*. 2010;32:405-410. doi:10.1016/j.gaitpost.2010.06.019
63. Martin HD, Palmer IJ. History and Physical Examination of the Hip: The Basics. *Curr Rev Musculoskelet Med*. 2013;6:219-225. doi:10.1007/s12178-013-9175-x
64. Martin HD, Kelly BT, Leunig M, et al. The Pattern and Technique in the Clinical

Evaluation of the Adult Hip: The Common Physical Examination Tests of Hip Specialists. *Arthrosc - J Arthrosc Relat Surg*. 2010;26(2):161-172. doi:10.1016/j.arthro.2009.07.015

65. Chadayammuri V, Garabekyan T, Bedi A, et al. Passive hip range of motion predicts femoral torsion and acetabular version. *J Bone Jt Surg - Am Vol*. 2016;98(2):127-134. doi:10.2106/JBJS.O.00334
66. Bryant JT, Reid JG, Smith BL, Stevenson JM. Method for determining vertebral body positions in the sagittal plane using skin markers. *Spine (Phila Pa 1976)*. 1989;14(3):258-265.
67. Mörl F, Blickhan R. Three-dimensional relation of skin markers to lumbar vertebrae of healthy subjects in different postures measured by open MRI. *Eur Spine J*. 2006;15(6):742-751. doi:10.1007/s00586-005-0960-0
68. Burnfield. JPJM. *Gait Analysis - Normal and Pathological Function*. Second. Thorofare: SLACK Incorporated; 2010.
69. Wong TKT, Lee RYW. Effects of low back pain on the relationship between the movements of the lumbar spine and hip. *Hum Mov Sci*. 2004;23(1):21-34. doi:10.1016/j.humov.2004.03.004
70. Lazennec J-Y, Charlot N, Gorin M, et al. Hip-spine relationship: a radio-anatomical study for optimization in acetabular cup positioning. *Surg Radiol Anat*. 2004;26(2):136-144. doi:10.1007/s00276-003-0195-x
71. Ellison JB, Rose SJ, Sahrmann SA. Patterns of hip rotation range of motion: a comparison between healthy subjects and patients with low back pain. *Phys Ther*. 1990;70(9):537-541. http://www.ncbi.nlm.nih.gov/pubmed/2144050. Accessed September 12, 2017.
72. Cibulka, Michael T. MHS/PT, OCS*; Sinacore, David R. PhD, PT†; Cromer, Gregory S. MS, PT‡; Delitto, Anthony PhD P. Unilateral Hip Rotation Range of Motion Asymmetry in Patients With Sacroiliac Joint Regional Pain. *Spine J*. 1998;23(9):971-1082.
73. Carriero A, Zavatsky A, Stebbins J, et al. Influence of altered gait patterns on the hip joint contact forces. *Comput Methods Biomech Biomed Engin*. 2012;17(4):1-8. doi:10.1080/10255842.2012.683575
74. Heller MO, Bergmann G, Deuretzbacher G, Claes L, Haas NP, Duda GN. Influence of femoral anteversion on proximal femoral loading: measurement and simulation in four

patients. *Clin Biomech (Bristol, Avon)*. 2001;16(8):644-649.

75. Carey TS, Crompton RH. The metabolic costs of 'bent-hip, bent-knee' walking in humans. *J Hum Evol*. 2005;48(1):25-44. doi:10.1016/j.jhevol.2004.10.001
76. Wilson DR, Feikes JD, O'Connor JJ. Ligaments and articular contact guide passive knee flexion. *J Biomech*. 1998;31(12):1127-1136. doi:10.1016/S0021-9290(98)00119-5
77. Whittle MW, Levine D. Three-dimensional relationships between the movements of the pelvis and lumbar spine during normal gait. *Hum Mov Sci*. 1999;18(5):681-692. doi:10.1016/S0167-9457(99)00032-9
78. Panjabi M, Yamamoto I, Oxland T, Crisco J. How does posture affect coupling in the lumbar spine? *Spine (Phila Pa 1976)*. 1989;14(9):1002-1011. doi:10.1097/00007632-198909000-00015
79. Oxland TR. Fundamental biomechanics of the spine-What we have learned in the past 25 years and future directions. *J Biomech*. 2015;49(6):817-832. doi:10.1016/j.jbiomech.2015.10.035
80. Pearcy M, Portek I, Shepherd J. The effect of low-back pain on lumbar spinal movements measured by three-dimensional X-ray analysis. *Spine (Phila Pa 1976)*. 1985;10(2):150-153.
81. Weitz EM. The lateral bending sign. *Spine (Phila Pa 1976)*. 6(4):388-397.
82. Roussouly P, Pinheiro-Franco JL. Biomechanical analysis of the spino-pelvic organization and adaptation in pathology. *Eur Spine J*. 2011;20 Suppl 5:609-618. doi:10.1007/s00586-011-1928-x
83. Roussouly P, Berthonnaud E, Roussouly D, et al. Sagittal morphology and equilibrium of pelvis and spine. *Eur Spine J*. 2002;(11):80-87.
84. Kong MH, Morishita Y, He W, et al. Lumbar Segmental Mobility According to the Grade of the Disc, the Facet Joint, the Muscle, and the Ligament Pathology by Using Kinetic Magnetic Resonance Imaging. *Spine (Phila Pa 1976)*. 2009;34(23):2537-2544. doi:10.1097/BRS.0b013e3181b353ea
85. Ward SR, Eng CM, Smallwood LH, Lieber RL. Are current measurements of lower extremity muscle architecture accurate? *Clin Orthop Relat Res*. 2009;467(4):1074-1082. doi:10.1007/s11999-008-0594-8

86. Ng KCGG, Rouhi G, Lamontagne M, Beaulé PE. Finite Element Analysis Examining the Effects of Cam FAI on Hip Joint Mechanical Loading Using Subject-Specific Geometries During Standing and Maximum Squat. *HSS J*. 2012;8(3):206-212. doi:10.1007/s11420-012-9292-x

87. Chegini S, Beck M, Ferguson SJ. The effects of impingement and dysplasia on stress distributions in the hip joint during sitting and walking: A finite element analysis. *J Orthop Res*. 2009;27(2):195-201. doi:10.1002/jor.20747